Åbo Akademi

OPEN ACCESS

This is an electronic reprint of the original article. This reprint may differ from the original in pagination and typographic detail.

Fatty Acid Epoxidation on Enzymes: Experimental Study and Modeling of Batch and Semibatch Operation

Wikström, Wilhelm ; Freites, Adriana; Tolvanen, Pasi; Lassfolk, Robert; Medina, Ananias; Eränen, Kari; Salmi, Tapio

Published in:
Industrial & Engineering Chemistry Research

DOI:
10.1021/acs.iecr.3c00890

Published: 14/06/2023

Document Version
Final published version

Document License
CC BY

Link to publication

Please cite the original version:
Wikström, W., Freites, A., Tolvanen, P., Lassfolk, R., Medina, A., Eränen, K., & Salmi, T. (2023). Fatty Acid Epoxidation on Enzymes: Experimental Study and Modeling of Batch and Semibatch Operation. *Industrial & Engineering Chemistry Research*, 9169-9187. https://doi.org/10.1021/acs.iecr.3c00890

General rights
Copyright and moral rights for the publications made accessible in the public portal are retained by the authors and/or other copyright owners and it is a condition of accessing publications that users recognise and abide by the legal requirements associated with these rights.

Take down policy
If you believe that this document breaches copyright please contact us providing details, and we will remove access to the work immediately and investigate your claim.

This document is downloaded from the Research Information Portal of ÅAU: 02. May. 2024

I&EC research
Industrial & Engineering Chemistry Research

pubs.acs.org/IECR

Article

Fatty Acid Epoxidation on Enzymes: Experimental Study and Modeling of Batch and Semibatch Operation

Published as part of the Industrial & Engineering Chemistry Research virtual special issue "Dmitry Murzin Festschrift".

Wilhelm Wikström, Adriana Freites Aguilera, Pasi Tolvanen, Robert Lassfolk, Ananias Medina, Kari Eränen, and Tapio Salmi*

Cite This: *Ind. Eng. Chem. Res.* 2023, 62, 9169–9187

Read Online

ACCESS | Metrics & More | Article Recommendations | Supporting Information

ABSTRACT: Biolubricants, plasticizers, bio-based rigid foams, and non-isocyanate polyurethanes can be made in a green way from epoxidized fatty acids. The classical technology for fatty acid epoxidation requires a reaction carrier, which acts as the real epoxidation agent. The process is complicated and involves a safety risk because of the appearance of percarboxylic acids. Therefore, the direct epoxidation of fatty acids in the presence of an immobilized enzyme is an attractive pathway to epoxidized fatty acids. Oleic acid was used as the model compound is this work, and commercial immobilized lipase Novozym 435 was used as the catalyst and hydrogen peroxide as the epoxidation agent. Batch and semibatch operation modes were tested in a laboratory-scale stirred tank reactor. The experimental results showed that almost complete conversions of the double bonds in oleic acid were achievable under isothermal batch and semibatch operation, with low concentrations of ring-opening byproducts. Semibatch operation gave an improvement of the product yield. Mathematical modeling of the experimental data was based on the reaction stoichiometry OA + HP → POA + W and OA + POA → EOA + OA, where OA = oleic acid, HP = hydrogen peroxide, POA = peroleic acid, W = water, and EOA = epoxized OA. Rate equations for the formation of peroleic acid and epoxide were derived, and the numerical values of the kinetic and adsorption parameters were estimated with nonlinear regression analysis. The reactor models consisted of ordinary differential equations, which were solved numerically during the parameter estimation until the optimal parameter values were reached. The model gave a very good description of the experimental data.

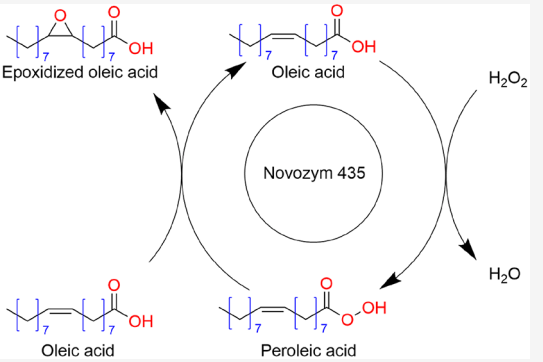

1. INTRODUCTION

During the past decades, the need for environmentally friendly alternatives to fossil-based raw materials has surged in chemical industry. This demand has led to new methods and techniques being developed for producing conventional products from different sources of biomass. Epoxidation of vegetable oils, such as palm oil, soybean oil, rapeseed oil, and sunflower oil, is a field actively being studied as a possible source of chemical intermediates.[1−4] These intermediates can be used for synthesis of chemical compounds, namely, alcohols, glycols, and olefinic compounds,[5] or for production of useful products, e.g., plasticizers, stabilizers, biolubricants, and non-isocyanate polyurethanes.[6−8]

With a projected increase in demand for vegetable oils and their derivatives, tall oil fatty acids (TOFAs) show a great promise as a sustainable source of nonedible vegetable oils in Northern European countries. Crude tall oil (CTO) is obtained as a side product of the well-known Kraft pulping process through pulping of soft- and hardwood.[9,10] Most vegetable oils consist of oleic acid and linoleic acid as the major components.[11] Furthermore, TOFA of good quality equates to 97% fatty acids consisting of up to 49.3% oleic acid and 45.1% linoleic acid.[12] In addition to extended research in the field of utilization of CTO by academia, there are major interest and investments by established companies such as Forchem, UOP, ENI, UMP, SunPine, Stora Enso, Neste, Haldor Topsoe, and Kraton.

Epoxidized vegetable oils are commercially produced via the Prileschajew epoxidation.[13] The Prileschajew method implies in situ formation of a percarboxylic acid, which is created in the aqueous phase through perhydrolysis of a carboxylic acid with hydrogen peroxide. The percarboxylic acid then diffuses into the

Received: March 17, 2023
Revised: May 11, 2023
Accepted: May 15, 2023
Published: June 2, 2023

Downloaded via 176.72.100.66 on December 21, 2023 at 06:26:16 (UTC).
See https://pubs.acs.org/sharingguidelines for options on how to legitimately share published articles.

ACS Publications

© 2023 The Authors. Published by American Chemical Society

https://doi.org/10.1021/acs.iecr.3c00890
Ind. Eng. Chem. Res. 2023, 62, 9169−9187

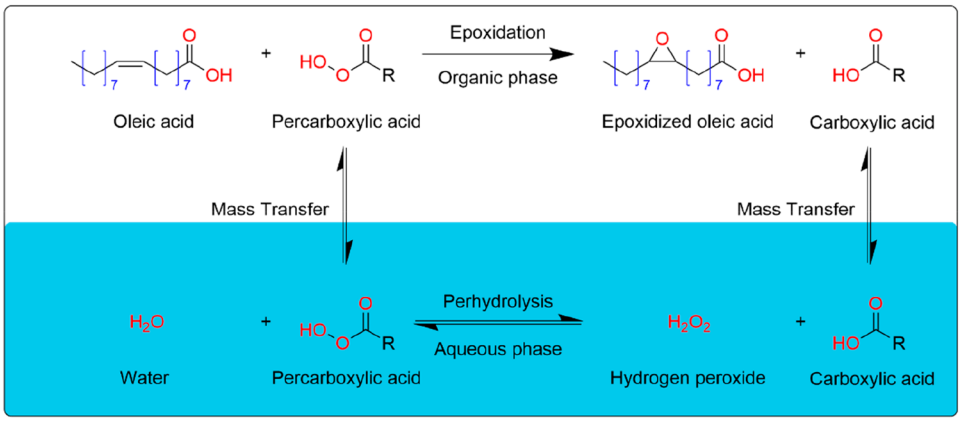

Figure 1. Prileschajew epoxidation of unsaturated fatty acid.

organic phase, where it reacts with the double bond of the unsaturated fatty acid, resulting in the epoxy group (the oxirane ring) and liberating the carboxylic acid. The carboxylic acid diffuses back to the aqueous phase, completing the reaction circle.[14−16] The reaction system is displayed in Figure 1.

The perhydrolysis is usually carried out in the presence of a strong homogeneous mineral acid catalyst such as hydrochloric acid, nitric acid, or sulfuric acid, with the last of these being the best-performing and most common one.[17] The drawback of using strong mineral acids as catalysts is the necessity to neutralize and remove the acid from the end products as well as the low selectivity due to side reactions where opening of the oxirane ring occurs as a consequence of the highly acidic conditions.[5,18] Because of these drawbacks, the use of acidic ion-exchange resins as heterogeneous catalysts has increased in popularity by virtue of their many advantages, namely, increased selectivity, suppression of undesirable side reactions, and easy separation from the end products, resulting in a more environmentally friendly method.[19,20]

A sufficient amount of research with metallic catalysts has been done, where catalysts such as titanium on amorphous silicon dioxide have shown high efficiency and exhibited no side reactions related to opening of the oxirane ring.[21] Furthermore, the use of methyltrioxomolybdenum and -rhenium as catalysts has demonstrated the lowest quantity of hydrogen peroxide needed and the shortest reaction time compared to conventional methods.[22,23] A few more unconventional methods have been proposed, e.g., epoxidation with the application of dioxiranes and epoxidation with the use of supercritical carbon dioxide.[24,25]

In recent years, a new trend has emerged where an enzymatic approach to epoxidation is utilized. What is special about the chemo-enzymatic approach is that there is no need for an additional carboxylic acid as the reaction carrier since the carboxylic group in the fatty acid takes that role. Björkling et al.[26] introduced the concept of using immobilized lipases for perhydrolysis of carboxylic acids and hydrogen peroxide to their corresponding percarboxylic acids. A few years later, Warwel and Rüsch gen. Klaas[27,28] introduced the concept of an in situ self-epoxidation of unsaturated fatty acids, where the enzymatically prepared unsaturated percarboxylic acid epoxidizes itself. The immobilized lipase used was *Candida antarctica* on polyacrylate resin (Novozym435).

The chemo-enzymatic method takes place in a liquid−liquid−solid system with hydrogen peroxide making up the aqueous phase, the lipase making up the solid catalyst, and the vegetable oil making up the organic phase. The lipase enzyme catalyzes the perhydrolysis, where the unsaturated fatty acid and hydrogen peroxide form the percarboxylic acid, which reacts with another unsaturated fatty acid, resulting in the epoxidized oil and an unsaturated fatty acid.[4] The reaction scheme for the chemo-enzymatic self-epoxidation is shown in Figure 2.

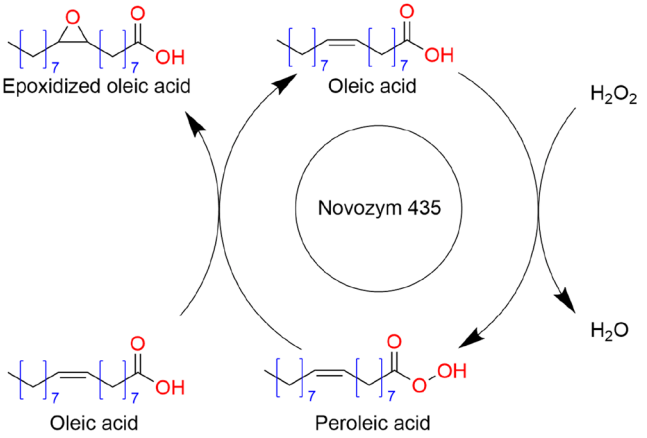

Figure 2. Reaction scheme for chemo-enzymatic epoxidation of oleic acid.

The chemo-enzymatic approach is favorable in several aspects, such as mild reaction conditions, high selectivity, and high conversion compared to conventional chemical methods. The high selectivity is mainly due to the low byproduct formation caused by ring opening. There is, however, a small amount of epoxy−peroxy acid formation as a consequence of the percarboxylic acid that is formed from the unsaturated fatty acid reacting with another identical peroxy acid.[29]

The lipase catalyst exhibits an excellent stability and activity, which has been proven by repeated reuse of the catalyst in epoxidation processes with high yields.[30] The substrate ratio, reaction temperature, and enzyme load affect the epoxidation significantly, since these are the key factors for increasing reaction rate and conversion, although a too-high enzyme load can be associated with agitation problems and decreased mass transfer.[31,32] In addition, it has been reported that the temperature and concentration of hydrogen peroxide have a great influence on the activity of the lipase catalyst.[33] At lower temperatures (∼20 °C) and moderate concentrations of hydrogen peroxide, there is no notable effect on enzyme activity. Likewise, at high temperatures (∼60 °C) without hydrogen

https://doi.org/10.1021/acs.iecr.3c00890
Ind. Eng. Chem. Res. 2023, 62, 9169−9187

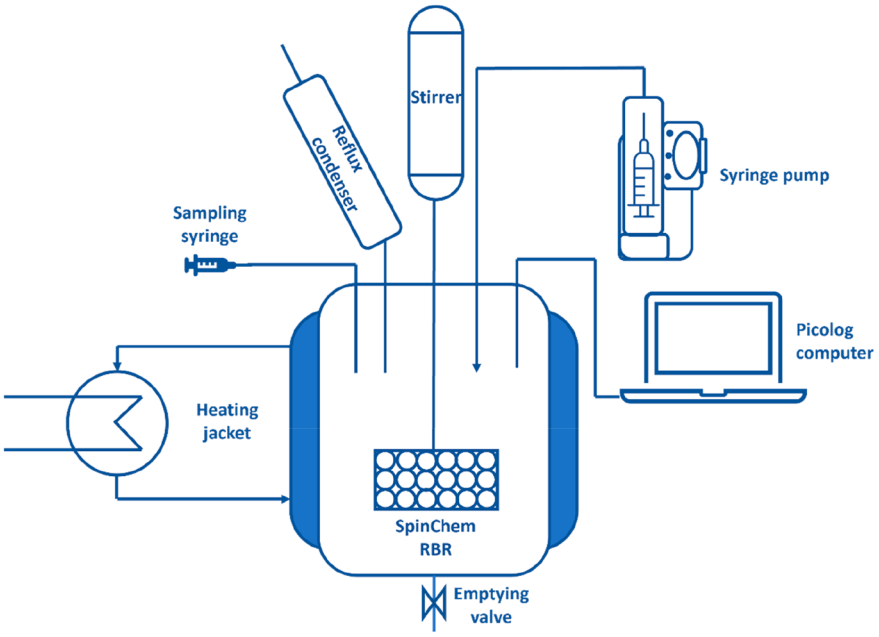

Figure 3. Scheme of the reactor system for fatty acid epoxidation.

peroxide the activity is well preserved. However, in a system with hydrogen peroxide, a linear decrease of the enzyme stability has been observed with an increase in hydrogen peroxide concentration or temperature.[34]

To combat the enzyme deactivation, an organic solvent is usually used to reduce the direct contact between the biocatalyst and hydrogen peroxide. Furthermore, a well-selected solvent will guarantee a good solubility of all substrates, increase the reaction kinetics, and limit the amount of substrate needed.[35] Toluene has been reported to be a suitable medium.[27,36] However, organic solvents are undesirable from the viewpoint of green chemistry.[37] The main point of improvement for solvent-free processes is the enzyme stability, which will make the process more cost-efficient and economically viable.[38,39]

Process intensification is a concept where novel technologies are applied to develop cleaner, safer, more compact, and more economical chemical processes. Common forms of process intensification involve different methods of stirring, heating, separation, etc. In the case of epoxidation, rotating bed reactors, microwave irradiation, and ultrasound irradiation are methods of process intensification with promising results,[15,40,41] In liquid−liquid systems, the mass transfer between the phases is of great importance. The SpinChem rotating bed reactor (RBR) can be implemented to minimize external mass transfer limitations by forced centrifugal flow through the hollow stirrer, where the catalyst is immobilized. Further benefits of the RBR technology are the protection of the catalyst from shear forces and grinding as well as simple separation and recycling of the catalyst from the reaction medium.[42−44]

The enzyme activity and stability are heavily affected by the hydrogen peroxide concentration and temperature.[34] To preserve the catalyst activity, the hydrogen peroxide contact with the catalyst should be limited. Since the use of organic solvents to protect the catalyst is ill-suited, alternative methods need to be investigated. Semibatch reactors operate similarly to batch reactors with the added modification of allowing the addition of reactants or removal of products over time. Semibatch reactors are generally used to control exothermic reactions or shift the reaction equilibrium through a purge stream. The investigation of semibatch technology in epoxidation has been very limited but promising.[45] The idea of utilizing semibatch reactors for the chemo-enzymatic epoxidation would be to continuously add hydrogen peroxide to the reaction mixture, thus keeping the hydrogen peroxide concentration low during the reaction. By keeping a low concentration of hydrogen peroxide throughout the reaction, the catalyst activity and stability should be preserved.

Oleic acid was selected as a model compound in this work. As catalyst the immobilized lipase Novozym435 was used, inducing mild reaction conditions without the need for an additional carboxylic acid for the reaction to occur. Additionally, the novel rotating bed and semibatch technologies were applied in this study. The ultimate aim was to intensify the epoxidation technology by combining enzymes, rotating bed technology, and semibatch operation.

2. EXPERIMENTAL EQUIPMENT AND PROCEDURES

2.1. Reactor Setup. All experiments were performed in a 250 mL glass reactor with an integrated heating jacket (Lenz). To prevent the escape of volatile compounds, a reflux condenser was installed above the reactor. For stirring the reaction mixture, the rotating bed reactor system (Spinchem RBR) was used. All experiments were conducted in batch or semibach modes. For the semibatch experiments, a syringe pump (Alaris Asena GS) was used for continuous addition of hydrogen peroxide. The experiments were performed under isothermal conditions, and the reaction temperature was monitored with a thermocouple. For withdrawal of samples, a 10 mL syringe was used. The reactor scheme can be found in Figure 3.

2.2. Chemicals and Experimental Matrix. All chemicals used were of commercial grade. The list of chemicals used with their purities and manufacturers can be found in the Supporting Information. In total 19 experiments were conducted. Generally, when performing kinetic experiments, the influence of temperature and stirring rate are investigated. These parameters were investigated in our previous work,[41] where the stirring rate was

https://doi.org/10.1021/acs.iecr.3c00890
Ind. Eng. Chem. Res. 2023, 62, 9169−9187

Table 1. Experimental Matrix

no.	catalyst loading (%)	OA:HP molar ratio	pumping time (h)[a]	temperature (°C)	stirring rate (rpm)	time (h)	goal
1	7	1:1	–	50	1000	6	repeatability
2	7	1:1	–	50	1000	6	molar ratio
3	7	1:2	–	50	1000	6	
4	7	1:3	–	50	1000	6	
5	10	1:3	–	50	1000	6	catalyst loading
6	13	1:3	–	50	1000	6	
7	4	1:3	–	50	1000	6	
8	7	1:3	6	50	1000	12	pumping time
9	7	1:3	7	50	1000	12	
10	7	1:3	10	50	1000	12	
11	7	1:3	20	50	1000	22	
12	7	1:1	–	50	1000	26	batch/semibatch
13	7	1:1	20	50	1000	26	
14	7	1:1	–	50	1000	8	deactivation batch
15	7	1:1	–	50	1000	8	
16	7	1:1	–	50	1000	8	
17	7	1:1	6	50	1000	8	deactivation semibatch
18	7	1:1	6	50	1000	8	
19	7	1:1	6	50	1000	8	
20	7	1:1		50	1000	8	deactivation[b]

[a]Batch experiments are marked with –. [b]Pretreatment of catalyst with hydrogen peroxide for 24 h.

varied between 500 and 1000 rpm and the reaction temperatures of 30−60 °C were screened. The stirring rates of 750 rpm and higher gave identical results,[41] indicating the removal of external mass transfer limitations around the catalyst particles; therefore, the stirring rate was fixed to 1000 rpm in the current work. In general, the attention of this work was shifted to the investigation of the catalyst loading and the hydrogen peroxide amount relative to fatty acid in batch mode and the influence of pumping time (the addition time of hydrogen peroxide) in semibatch mode. A substantial number of experiments in both batch and semibatch modes were focused on deactivation of the catalyst, where three consecutive experiments with reused catalyst were performed in each mode. The experiments along with their reaction conditions are listed in Table 1.

2.3. Experimental Procedures. All experiments were conducted in the same reactor setup. Desired amounts of oleic acid, hydrogen peroxide, water, and lipase (Novozym 435) were weighed in separate flasks and beakers. Oleic acid, water, and lipase were added to the reactor, after which heating and stirring were turned on to reach the desired temperature. The SpinChem RBR was used as a stirrer to form the emulsion with the catalyst added to the reaction mixture instead of loading it into the RBR chamber. After the reaction mixture reached the desired temperature, hydrogen peroxide was slowly added to the reactor over a 1 min time period. This was done to reduce any temperature fluctuations and spare the lipase stability from the initial impact. This procedure was applied in all the experiments performed in batch mode. In cases where the experiments were conducted in semibatch mode, the pump was turned on after reaching the desired temperature, initiating the dosing of hydrogen peroxide. When the first drop of hydrogen peroxide was added to the reaction mixture was when the reaction and the experiment were deemed to have begun. Different addition times of hydrogen peroxide were used to investigate the effect of semibatch operation (Table 1).

After the reaction was carried out to the desired point, stirring was turned off, and the reaction mixture was drained out of the reactor. In cases where the lipase reusability was investigated, the reaction mixture was left in the reactor for 30 min to let the emulsion separate into two separate phases. The aqueous phase was withdrawn, and toluene was added to the remaining organic phase for ease of handling. The organic phase was withdrawn, and the lipase enzyme was recovered through vacuum filtration. The enzyme was then left in toluene under stirring to further remove any possible reactants or products that could be remaining. Thereafter, the lipase was once again filtered and left to dry in a fume hood for at least 48 h before being reused in the next reaction.

2.4. Analytical Methods for Reactants and Products. Samples were withdrawn typically every hour, but the interval between sampling increased the longer the experiment lasted. The samples were withdrawn with a 10 mL plastic syringe through a Teflon-coated sampling tube. The volume of the samples was 4 mL, except for the third deactivation experiments, where the reaction volume was significantly lower. The sample was deposited in an 8 mL sample bottle, which was then placed in a centrifuge to separate the phases. Pasteur pipettes were used to separate the two phases into separate 4 mL vials. The hydrogen peroxide and oxirane number analyses were performed within 30 min of the sample being withdrawn to prevent decomposition of hydrogen peroxide and to avoid solidification of the organic phase and the problems associated with it. The hydrogen peroxide content, the concentration of double bonds (iodine value), and the concentration of epoxide groups (oxirane number) were determined by titrimetric methods. For hydrogen peroxide analysis, the method of Greenspan and MacKellar[46] was used, whereas the Hanus method[47,48] gave the iodine value and Jay's method[49] gave the oxirane number. The experimental error in the titrimetric analysis was confirmed to be low, less than 5%, as samples were analyzed repeatingly, but because of the sample pretreatment, some analytical values deviated more. The details of the titrimetric analyses are described in the Supporting Information. Nuclear magnetic resonance spectroscopy (NMR) was used to analyze the composition of the oleic acid and the products in the organic phase. The equipment used was a Bruker AVANCE III

https://doi.org/10.1021/acs.iecr.3c00890
Ind. Eng. Chem. Res. 2023, 62, 9169−9187

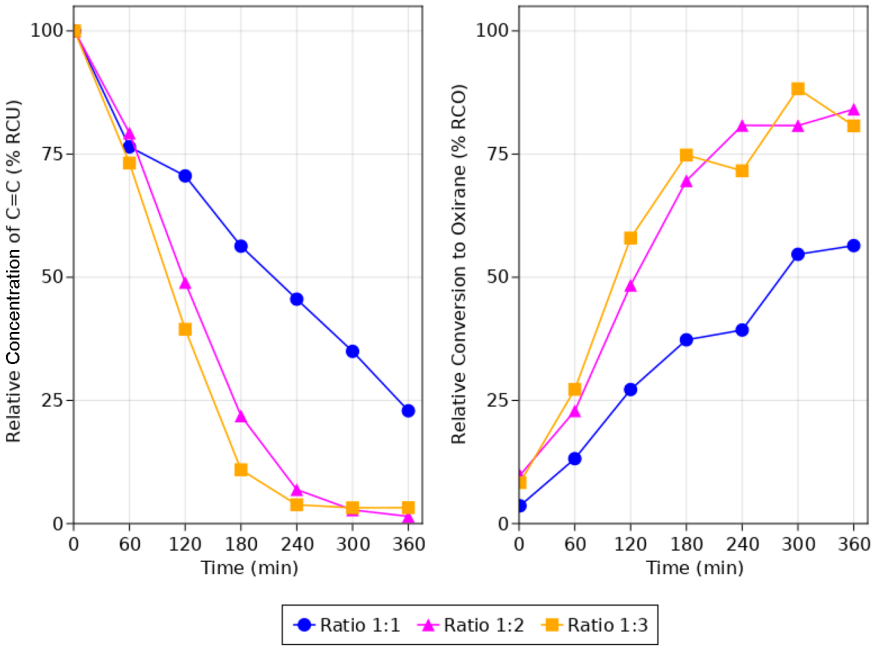

Figure 4. Relative concentration of double bonds (RCU) (dimensionless concentration) and relative conversion to oxirane (RCO) for different OA:HP molar ratios during a 6 h period.

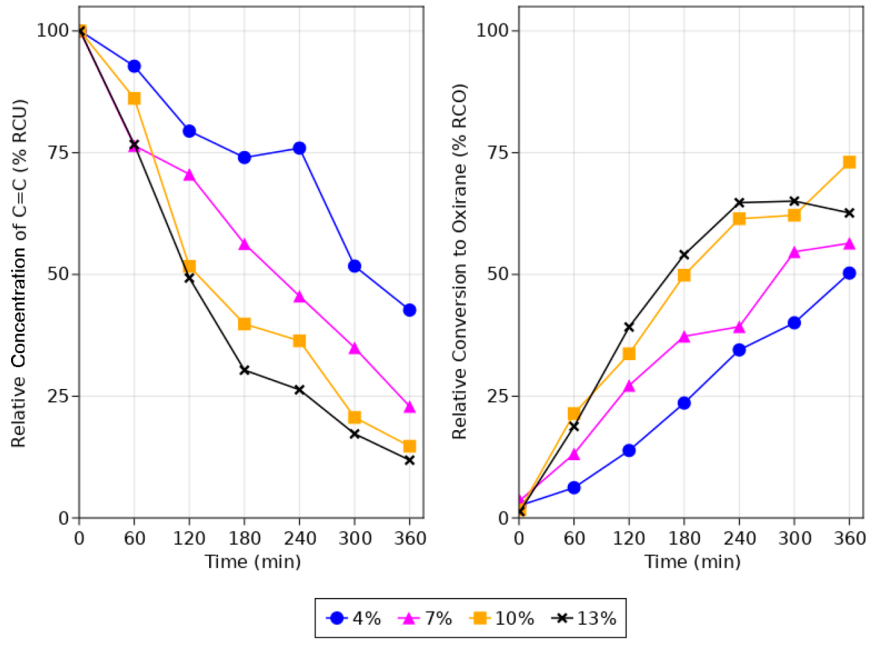

Figure 5. Relative concentration of double bonds (RCU) and relative conversion to oxirane (RCO) for different catalyst loadings during a 6 h period.

spectrometer. The accuracy of the NMR studies was confirmed by repeated analysis and comparing oleic acid standards (see the Supporting Information). The variance of identical repeated NMR analysis was maximally 2%.

2.5. Catalyst Analysis. For analyzing the morphology and any potential mechanical or corrosive damage on the catalyst, scanning electron microscopy (SEM) was used. The model of the equipment was a Zeiss Leo Gemini 1530, and the images were taken at 30×, 100×, 250×, 1000×, 5000×, and 10000× zoom. Nitrogen physisorption was used to analyze the specific surface area of the fresh lipase catalyst as well as lipase catalyst used in successive batch and semibatch experiments. The equipment used was a Micromeritics 3Flex-3500 adsorption analyzer. Before the measurements, the catalysts were outgased under vacuum at 50 °C for 24 h. For calculating the specific surface area of the catalyst, the BET equation was used.

3. EXPERIMENTAL RESULTS AND DISCUSSION

3.1. Hydrogen Peroxide Amount. The influence of hydrogen peroxide was studied with batchwise experiments by varying the amount of hydrogen peroxide compared to the unsaturated fatty acid. The oleic acid to hydrogen peroxide (OA:HP) molar ratios studied were 1:1, 1:2, and 1:3. A 30% w/w hydrogen peroxide solution was used for the following

https://doi.org/10.1021/acs.iecr.3c00890
Ind. Eng. Chem. Res. 2023, 62, 9169−9187

experiments with a fixed catalyst load of 7% w/w of fatty acid. The reaction temperature was kept at 50 °C and stirring at 1000 rpm using the Spinchem RBR. The reactions were performed for 6 h with samples being withdrawn every hour. The results from the experiments are displayed in Figure 4.

The experimental results revealed that the conversion of double bonds and yield of oxirane are heavily affected by the ratio OA:HP. Furthermore, the rate at which a high conversion is reached is higher for higher concentrations of hydrogen peroxide. The difference between the 1:1 and 1:2 OA:HP ratios are quite significant, whereas the difference between 1:2 and 1:3 OA:HP ratios are minor, as can be seen in Figure 4. This issue was considered further by mathematical modeling of the reaction mechanism and kinetics (sections 4.2−4.4). In our previous work,[41] an OA:HP ratio of 1:1.5 performed almost as well as an OA:HP ratio of 1:2 after 6 h and 12 h of reaction, but comparing the overall results, a higher relative conversion to oxirane (RCO) was achieved in this work for all molar ratios tested. In previous studies, byproducts due to ring-opening reactions have been observed,[15,41,42] By looking at Figure 4, it can be seen that some kind of side reactions or ring opening takes place. It has been previously reported that high amounts of hydrogen peroxide negatively affect the activity of the lipase catalyst at temperatures exceeding 20 °C.[34] This was not observed in our experiments, but that could be due to the relatively low concentration of the hydrogen peroxide solution used (30% w/w), resulting in quite a diluted system.

3.2. Catalyst Loading. The effect of catalyst loading on the reaction was investigated by varying the catalyst amount with respect to the amount of unsaturated fatty acid. Batchwise operation was applied. The catalyst loadings studied were 4%, 7%, 10%, and 13% w/w of fatty acid. The molar ratio between hydrogen peroxide and oleic acid was set to 1:1 for all the experiments for a straightforward analysis without the interference of other variables. The temperature was set to 50 °C and stirring rate to 1000 rpm for all the experiments. Samples were withdrawn every hour, and after 6 h of reaction time the experiments were ended.

Figure 5 shows a quite clear trend of increased conversion and yield in relation with an increased catalyst amount. There seems to be a deviation to the trend, with the 10% catalyst loading achieving higher RCO than 13%; this is however most likely an outlier data point due to analytical error. Comparing the 4% to the 13% catalyst loading reveals an increase in yield of only around 25% for over 3 times the amount of catalyst. The immobilized lipase catalyst used in these experiments is a novel catalyst and because of that quite an expensive one. Because of this, the small gain in yield would not necessarily justify the cost of adding more catalyst, especially in our case with its tendency to deactivate in absence of an organic solvent.

As shown in Figure 6, by plotting RCO versus a combined variable of reaction time multiplied by catalyst mass, the graphs start to overlap quite well, which indicates that the multiphase system might be kinetically controlled, i.e., the interfacial mass transfer limitations are negligible. This confirms the observations made in our previous work[41] that 1000 rpm is a stirring rate which guarantees the absence of external mass transfer limitations around the particles.

3.3. Semibatch Operation: Gradual Addition of Hydrogen Peroxide. The influence of addition of hydrogen peroxide to the reactor vessel was studied by continuously adding 30% w/w hydrogen peroxide solution to the reaction in a semibatch system. In the beginning of the reaction, no hydrogen

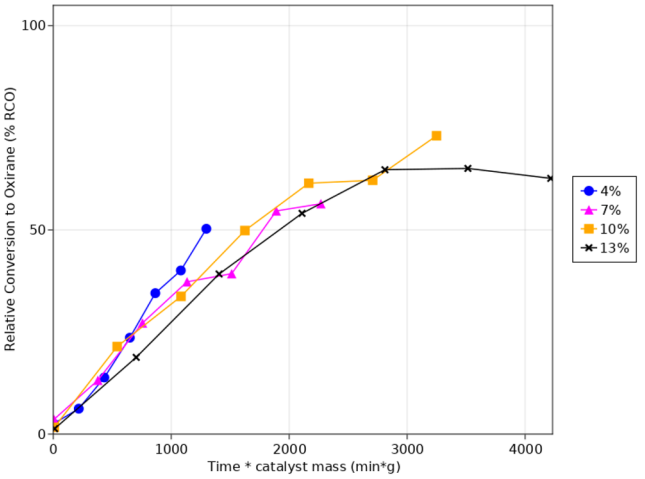

Figure 6. Relative conversion to oxirane (RCO) as a function of reaction time multiplied by catalyst mass.

peroxide was present in the liquid phase. The OA:HP molar ratio for the semibatch experiment was 1:3. The high molar ratio was selected due to the fact that the effect of the semibatch addition would be more prominent or visible at higher hydrogen peroxide concentrations. Four different pumping rates were tested (addition times of 6, 7, 10, and 20 h) to achieve the initial 1:3 molar ratio. After stopping the addition of hydrogen peroxide, the reaction was conducted in batch mode until a total reaction time of 12 h had been reached. An exception to this was the 20 h addition time experiment, which was continued in batch mode for an additional 2 h for a total reaction time of 22 h. The other reaction conditions for the experiments were the temperature of 50 °C and the stirring speed of 1000 rpm. All the experiments had a final double-bond conversion of close to 100%.

A molar ratio of 1:1 OA:HP was used in subsequent experiments. Furthermore, to keep a low concentration of hydrogen peroxide in the reaction and to avoid the "quasi-batch system from the previous experiments, a 20 h addition time was chosen. After turning off the pump, the experiment proceeded in batch mode for an additional 6 h for a total reaction time of 26 h. Parallel experiments in batch mode were also performed for the sake of comparison. The temperature and stirring rate were kept the same as the previous experiments. The results for these experiments can be seen in Figures 7−9. All the experiments had a final double-bond conversion of close to 100%, which can be seen in Figure 7.

With this approach, good results were obtained. The hydrogen peroxide concentration was kept low during the semibatch experiments, as shown in Figure 8. After 26 h of reaction time, the semibatch approach resulted in a higher yield with a minimal difference in conversion of double bonds, as can be seen in Figures 7 and 9. This indicates that the semibatch approach decreased ring-opening reactions. Although a higher oxirane yield was achieved with the semibatch mode, it is still difficult to justify the approach from an industrial viewpoint due to the long reaction time required. The epoxide yield at around 18 h in semibatch mode was achieved within 6 h in batch mode. By increasing the catalyst loading, the reaction time could be shortened, whereas the increase of the reaction temperature can lead to loss of hydrogen peroxide by decomposition. However, in laboratory scale and research efforts, the semibatch approach

https://doi.org/10.1021/acs.iecr.3c00890
Ind. Eng. Chem. Res. 2023, 62, 9169−9187

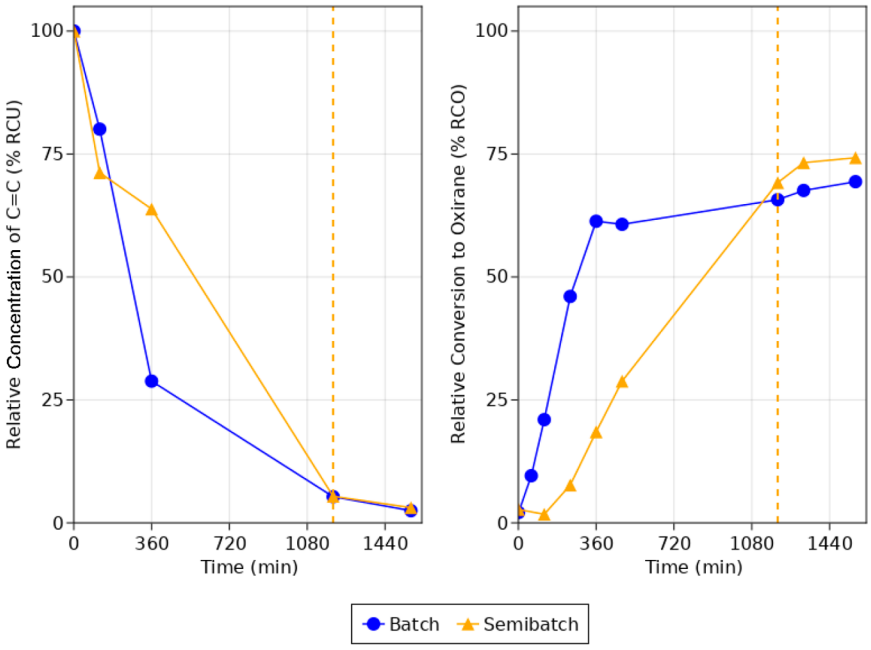

Figure 7. Comparison of relative concentration of double bonds (RCU) and relative conversion to oxirane (RCO) between batch and semibatch modes. Dotted lines indicate the time at which the addition of hydrogen peroxide was stopped in semibatch operation.

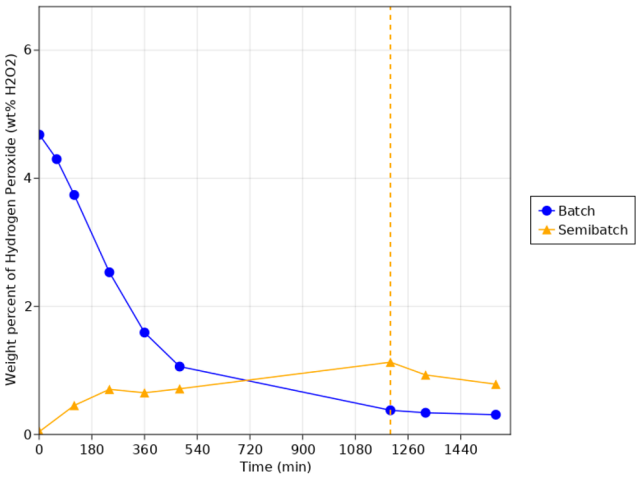

Figure 8. Comparison of hydrogen peroxide concentration over time for different addition times of hydrogen peroxide. Dotted lines indicate the time at which the addition of hydrogen peroxide was stopped in semibatch mode.

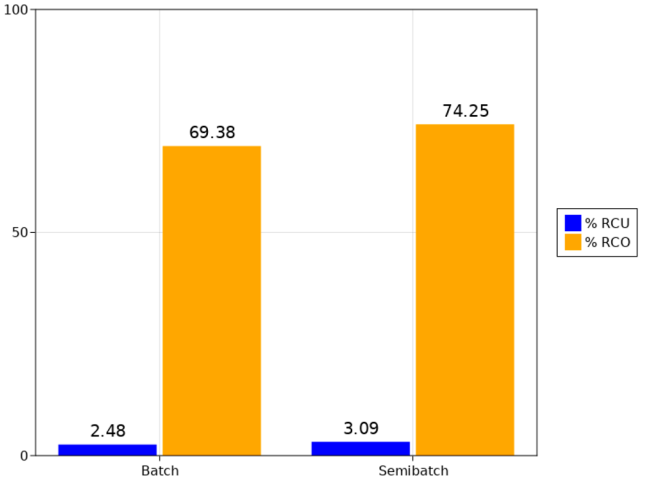

Figure 9. Comparison of relative concentration of double bonds (RCU) and relative conversion to oxirane (RCO) between batch and semibatch modes at 26 h.

can be beneficial, since the low reaction rate and long reaction time are ideal for intrinsic kinetic measurements.

3.4. Catalyst Durability. It is well-known that hydrogen peroxide can have a negative effect on the catalyst activity.[33] Despite this, many studies have been able to perform several consecutive experiments using the same catalyst with a negligible toll on the catalyst stability and activity. This has been possible by using an organic solvent to protect the catalyst by reducing the direct contact with hydrogen peroxide.[27,30,36] However, most of the organic solvents are not environmentally friendly and are problematic to handle in industrial settings, and therefore, they should be avoided. Because of this, the interest of this work was shifted to studying the catalyst activity and stability in a solvent-free medium using a semibatch approach.

Both batch and semibatch experiments were conducted. The reaction temperature was kept at 50 °C, operating within the range of optimum usage conditions for the catalyst. The stirring speed was kept at 1000 rpm to operate within the kinetic regime, and an OA:HP molar ratio of 1:1 was selected based on the new understanding from the semibatch experiments. This time, the reaction time was fixed to 8 h. For the experiments where the semibatch approach was used, hydrogen peroxide was continuously added for 6 h, whereafter the reaction was allowed to continue for another 2 h in batch mode. After each experiment, the catalyst was recovered through vacuum filtration, washed with toluene, and left to dry for 48 h in a fume hood. To compensate for the loss of some small catalyst amounts during recovery, the reactant quantities were adjusted for each experiment to keep the same proportions in all

https://doi.org/10.1021/acs.iecr.3c00890
Ind. Eng. Chem. Res. 2023, 62, 9169−9187

experiments. In total the catalyst was used for three consecutive experiments for each approach.

Figures 10 and 11 summarize and compare the successive experiments reusing the lipase catalyst. A clear trend in catalyst

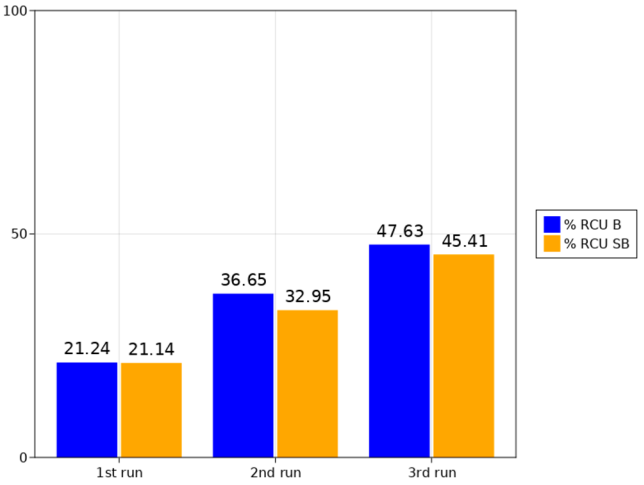

Figure 10. Relative concentration of double bonds (RCU) at 8 h for three consecutive experiments reusing the same catalyst in batch (B) and semibach (SB) mode.

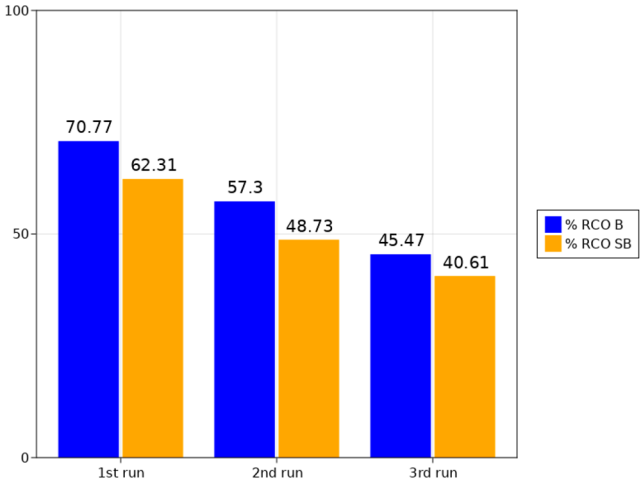

Figure 11. Relative conversion to oxirane (RCO) at 8 h for three consecutive experiments reusing the same catalyst in batch (B) and semibach (SB) mode.

deactivation can be seen for both the batch and semibatch approaches. Unlike the 20 h addition time experiment, the results for batch and semibatch are very comparable. This is likely due to the much shorter addition time of hydrogen peroxide. What is surprising is that although the hydrogen peroxide amount in the semibatch system stayed way below that of the batch system for the majority of the experiments, the final relative concentration of double bonds (RCU) and RCO values, which can be seen in Figures 10 and 11, were not far off each other. This would indicate that at these levels of hydrogen peroxide in the system, the catalyst stability is rather similar. This raises the question of how big of an impact hydrogen peroxide has on the catalyst stability and activity overall and what other factors might contribute to the catalyst deactivation.

To further investigate how much of an impact hydrogen peroxide has on the catalyst stability and activity, a subsequent experiment was performed where the lipase catalyst was pretreated with hydrogen peroxide. The catalyst was treated by leaving it in a 30% w/w hydrogen peroxide solution for 24 h before carrying out an experiment with similar conditions to the previous deactivation experiments. After the 24 h the catalyst was rinsed with water to remove any excess hydrogen peroxide and then left to dry overnight in the fume hood before being used for the experiment. The experiment was conducted in a batch system at 50 °C and 1000 rpm. A comparison between the consecutive experiments reusing the catalyst and the experiment with the pretreated catalyst can be seen in Figures 12 and 13.

As expected, the pretreatment of the catalyst with 30% w/w hydrogen peroxide solution affected the activity to a high extent, which can be seen by comparing the results from the first run with non-pretreated catalyst and the run with preatreated catalyst in Figure 13. The pretreated catalyst was exposed to high concentrations of hydrogen peroxide for 24 h in addition to 8 h of reaction time, whereas the non-pretreated catalyst was only exposed to relatively low concentrations of hydrogen peroxide for the three successive reactions for a total of 24 h. Taking this into consideration, a future challenge would be to investigate in which way hydrogen peroxide deactivates the lipase catalyst.

3.5. NMR Analysis of Unsaturated Fatty Acid and Reaction Products. NMR was used to analyze the unsaturated fatty acid as well as the reaction products of the epoxidation. Two different oleic acids from different suppliers were utilized in the experiments. The purity of these chemicals was given with quite a generous range, and because of that, NMR analysis was performed to better compare their composition. The ^{1}H NMR spectra for the two oils are given in the Supporting Information. Only minimal differences between the oils were observed from the ^{1}H NMR spectra, which is important for the consistency of the experimental data. Both oils contained about 6% linoleic acid, and the stearic acid content was estimated to be around 10%.

Besides the two oils, the reaction products were analyzed for two experiments. The samples used for the analysis were from the experiments comparing the batch and semibatch approaches with an OA:HP molar ratio of 1:1 with a 20 h addition time of hydrogen peroxide in the semibatch experiment. The conditions for the experiments can be seen in Table 1 (experiments 12 and 13), and the comparison between the experimental results can be seen in Figures 7−9. The ^{1}H NMR spectra highlighting relevant compounds from the experiments can be seen in Figure 14 and are complemented by Table 2, which displays the numerical comparison between the compound fractions (B = batch experiment, SB = semibatch experiment).

These spectra confirm the observations from the kinetic experiments. The reaction taking place in the batch reactor progressed much more rapidly than the one taking place in the semibatch reactor, which can be seen in the differences of sizes of the peaks for the alkane and epoxide groups at 8 h. This is, of course, to be expected because of the much higher concentration of hydrogen peroxide at the beginning of the experiment in batch mode, increasing the likelihood of the reaction occurring. At 26 h most of the alkene groups had reacted for both approaches. However, the amount of epoxide was significantly higher in the sample from the semibatch experiment than that of the batch experiments, 76.9% compared to 65.9% respectively. The epoxide content for the batch sample had even decreased from 69.6% at 8 h to 65.9% at 26 h.

The reason for the decrease of the oxirane content is ring-opening reactions, implying that there is an optimal time for

https://doi.org/10.1021/acs.iecr.3c00890
Ind. Eng. Chem. Res. 2023, 62, 9169−9187

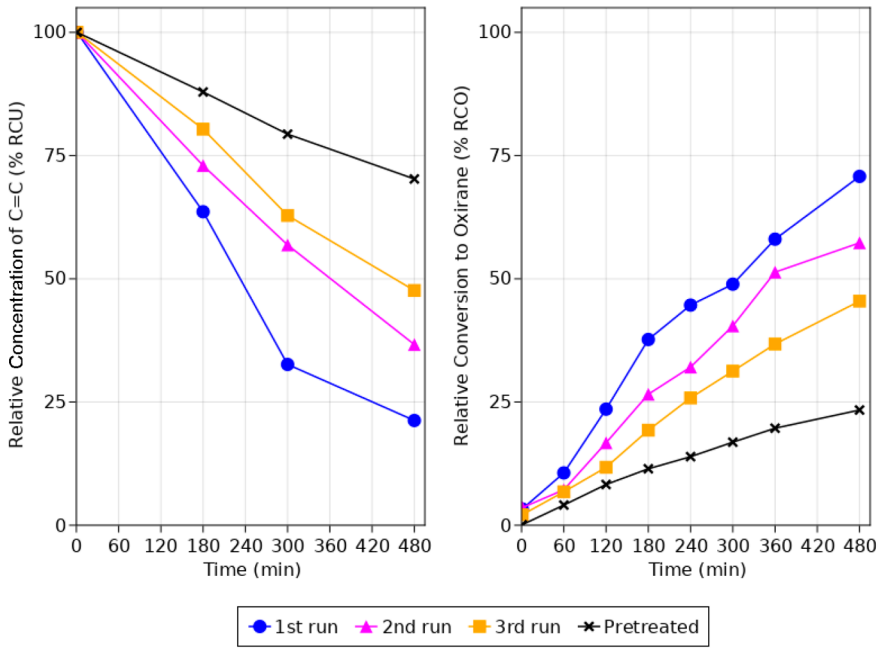

Figure 12. Comparison of relative concentration of double bonds (RCU) and relative conversion to oxirane (RCO) for three consecutive experiments reusing the same catalyst in batch mode and a single experiment using a catalyst pretreated with 30% w/w hydrogen peroxide solution for 24 h.

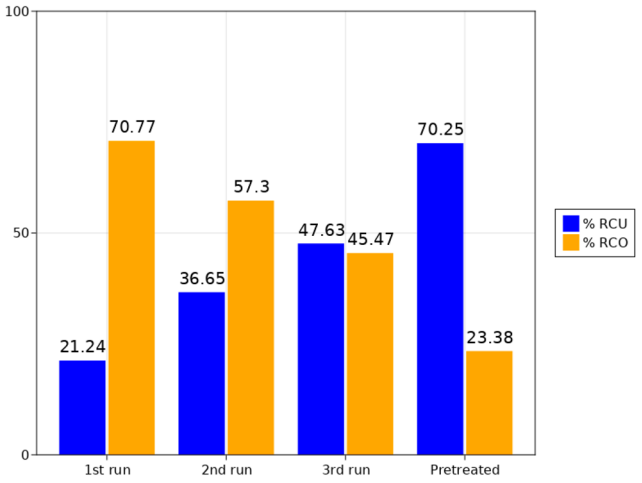

Figure 13. Comparison of relative concentration of double bonds (RCU) and relative conversion to oxirane (RCO) at 8 h of reaction time for three consecutive experiments reusing the same catalyst in batch mode and a single experiment using a catalyst pretreated with 30% w/w hydrogen peroxide solution for 24 h.

maximum yield before ring-opening reactions start eating more products than are produced. As a result of the ring-opening reactions, some ring-opening products appear in the NMR spectra in the form of diols and esters, with diols being the dominant ones. Some amounts of ring-opening products can be seen in each sample, with diols appearing at a 2:1 ratio of esters. Quite the opposite was observed for the ring-opening products in a previous work,[41] with esters dominating over diols with a ratio of 1:0.4.

Overall, less ring-opening products were observed in the semibatch samples. At 26 h the ring-opening products make up quite a substantial part of the sample at 30% for the batch approach and around 22.5% for the semibatch approach. Semibatch operation has a clearly positive effect on the epoxide selectivity. Even though linoleic acid, besides oleic acid, is present as a minor component in the reactant, the NMR studies did not find any epoxidized mono- or dilinoleic acids (diepoxystearic acid), since the concentrations were too low.

3.6. Catalyst Characterization: SEM and Nitrogen Physisorption. To analyze any changes of the catalyst morphology due to potential mechanical and/or corrosive damages, scanning electron microscopy (SEM) was used. Fresh catalyst was compared to catalysts that had been reused in three consecutive experiments in batch and semibatch modes as well as the catalyst pretreated with 30% w/w hydrogen peroxide solution for 24 h. SEM images were taken at 30×, 100×, 250×, 1000×, 5000×, and 10000× zoom. The most relevant images can be found in the Supporting Information.

At 30× zoom, no immediate differences can be spotted between any of the catalyst particles from the different samples. At 100× zoom, the pretreated catalyst looks as good as the fresh one. The reused catalysts on the other hand seem to have small changes on their surfaces compared to the fresh catalyst. This is, however, because of some mechanical damages caused by the stirring. The same pattern follows for the 250× zoom, with little changes for the pretreated catalyst and some mechanical damages on the reused ones. No qualitative changes can be observed in the morphology of the particles is solely based on these images.

To better understand the changes in the catalyst performances, nitrogen physisorption was conducted. The BET surface area for each sample can be seen in Table 3. The surface area of the reused catalysts decreased significantly. Since the SEM images revealed miniscule changes in the morphology, it is easy to attribute the decrease in surface area to some sort of deposition clogging the pores of the catalyst. The pretreated sample could not give a definitive result for the surface area because it was too low or there were solidified products that melted during the analysis. The differences in the surface areas between the catalysts used in the batch experiments versus the semibatch experiments are quite considerable. From the kinetic

https://doi.org/10.1021/acs.iecr.3c00890
Ind. Eng. Chem. Res. 2023, 62, 9169−9187

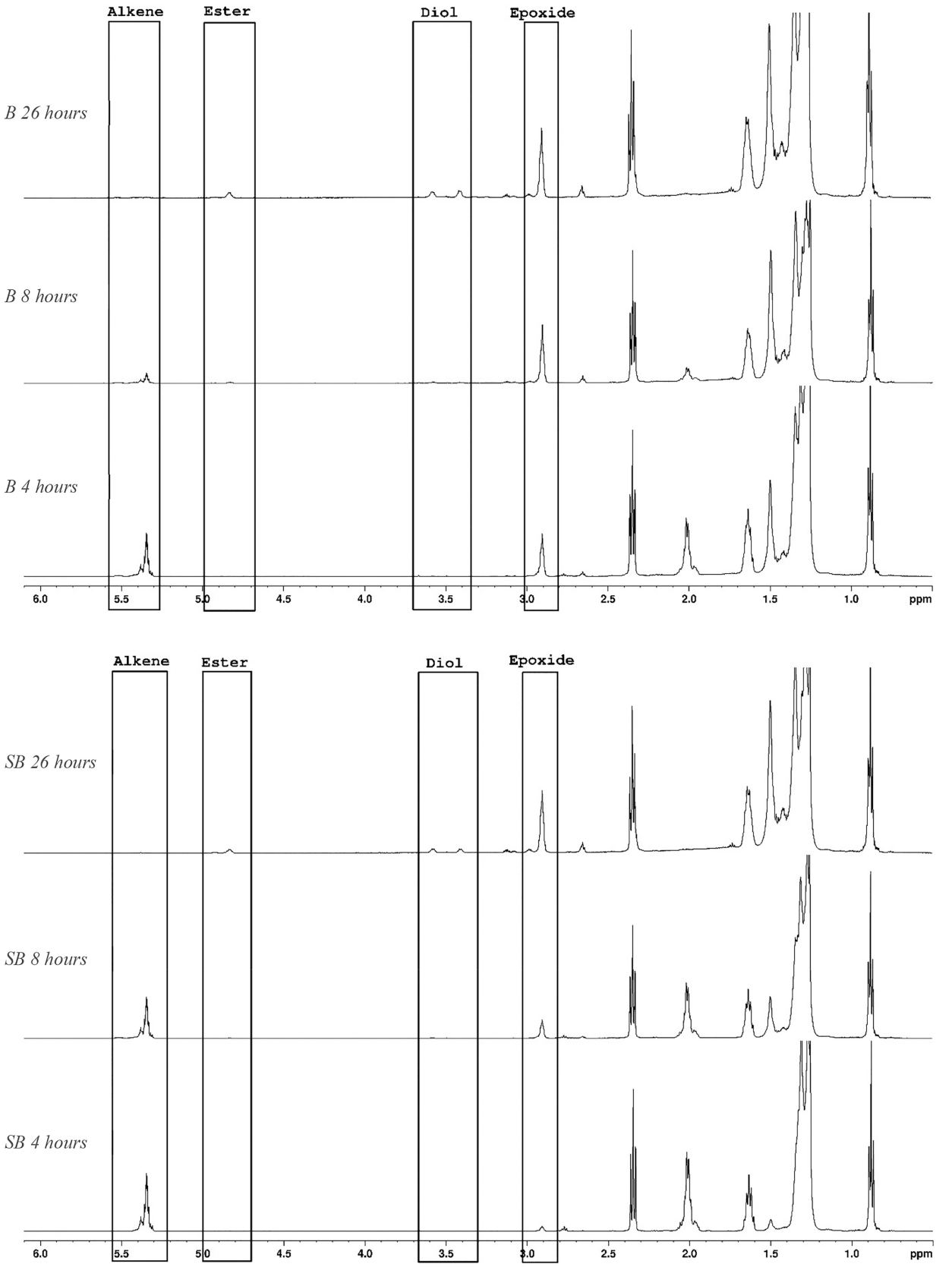

Figure 14. ^{1}H NMR spectra comparing the reaction products for experiments performed in batch (B) and semibatch (SB) modes.

experiments and NMR analysis it is already clear that the semibatch approach impedes the formation of ring-opening products while producing similar yields for the epoxide. With this in mind it could be concluded that the ring-opening

https://doi.org/10.1021/acs.iecr.3c00890
Ind. Eng. Chem. Res. 2023, 62, 9169−9187

Table 2. Compound Fractions Determined by ^{1}H NMR

sample	alkene	epoxide	hydroxyl	ester
B 4 h	0.484	0.425	0.00645	0.00645
B 8 h	0.157	0.697	0.0449	0.02247
B 26 h	0.0231	0.659	0.208	0.09249
SB 4 h	0.919	0.0753	0.00538	0
SB 8 h	0.702	0.281	0.0112	0.00562
SB 26 h	0.00578	0.769	0.150	0.0751

Table 3. BET Surface Areas of Fresh, Pretreated, and Reused Catalysts

sample	BET surface area (m^2/g)
fresh catalyst	51.3
pretreated catalyst	N/A
reused catalyst in batch experiment	9.9
reused catalyst in semibatch experiment	17.5

products are the most probable cause of the blocking of catalyst pores rather than the epoxide itself.

4. MODELING OF BATCH AND SEMIBATCH EPOXIDATION PROCESSES

4.1. Reaction Stoichiometry. Different proposals for the enzymatic epoxidation of unsaturated fatty acids have been given, and they were thoroughly discussed and compared in a recent article.[50] The underlying question that has been up for discussion is whether the percarboxylic acid, formed after the perhydrolysis, occurs only briefly before being consumed or accumulates in the system. If the peracid only exists briefly in the reaction system, a simplification can be made, where direct epoxidation between the unsaturated fatty acid and hydrogen peroxide is assumed.[28,29]

If the reaction proceeds via the percarboxylic acid route, the overall stoichiometry is

$$\mathrm{OA + HP \rightarrow POA + W} \quad \text{(I)}$$

$$\mathrm{POA + OA \rightarrow EOA + OA} \quad \text{(II)}$$

$$\mathrm{POA + POA \rightarrow EPOA + OA} \quad \text{(III)}$$

which is illustrated in Figure 15. The simplified alterative is the direct epoxidation between the unsaturated fatty acid and hydrogen peroxide:

$$\mathrm{OA + HP \rightarrow EOA + W} \quad \text{(IV)}$$

which is visualized in Figure 16.

4.2. Reaction Mechanism and Rate Equation. In a previous work of our group,[50] different mechanisms and models for enzymatic epoxidation of oleic acid were thoroughly investigated. For this work, the best performing and most accurate model from the mentioned work was used and modified, although the differences between the models were nominal. This model uses the Langmuir−Hinshelwood concept to describe the interactions of the molecules with the catalyst surface. The molecules absorb on the vacant sites of the catalyst, where they react and form the products that posteriorly desorb from the catalyst. It is assumed that all components occupy only one basic site on the catalyst surface, which gives the mechanistic sequence shown in Table 4.

The quasi-equilibrium approximation can be applied to the adsorption and desorption steps because they are rapid in comparison to the rate-determining steps (rds). The generation rates can therefore be described as follows:

$$r_{\mathrm{I}} = k_{\mathrm{I}}\theta_{\mathrm{OA}}\theta_{\mathrm{HP}} \quad (1)$$

$$r_{\mathrm{II}} = k_{\mathrm{II}}\theta_{\mathrm{OA}}\theta_{\mathrm{POA}} \quad (2)$$

$$r_{\mathrm{III}} = k_{\mathrm{III}}\theta_{\mathrm{POA}}^{\,2} \quad (3)$$

where θ is the fraction of adsorbed molecules on active surface sites on the catalyst. The equilibrium constant for the adsorption and desorption quasi-equilibria steps can be expressed as

$$\theta_i = K_i c_i \theta_{\mathrm{v}} \quad (4)$$

where θ_i is the fraction of absorbed molecule on active sites of the catalyst, θ_{v} is the fraction of vacant surface sites, and c_i is the concentration in the liquid phase. By taking the sum of all fractions of molecules adsorbed on active sites ($\sum\theta_i$) and adding the fraction of vacant surface sites (θ_{v}) we obtain

$$\theta_{\mathrm{v}} + \sum \theta_i = 1 \quad (5)$$

By combining eqs 4 and 5, we arrive at an expression that can be used for calculating the fraction of vacant sites (θ_v):

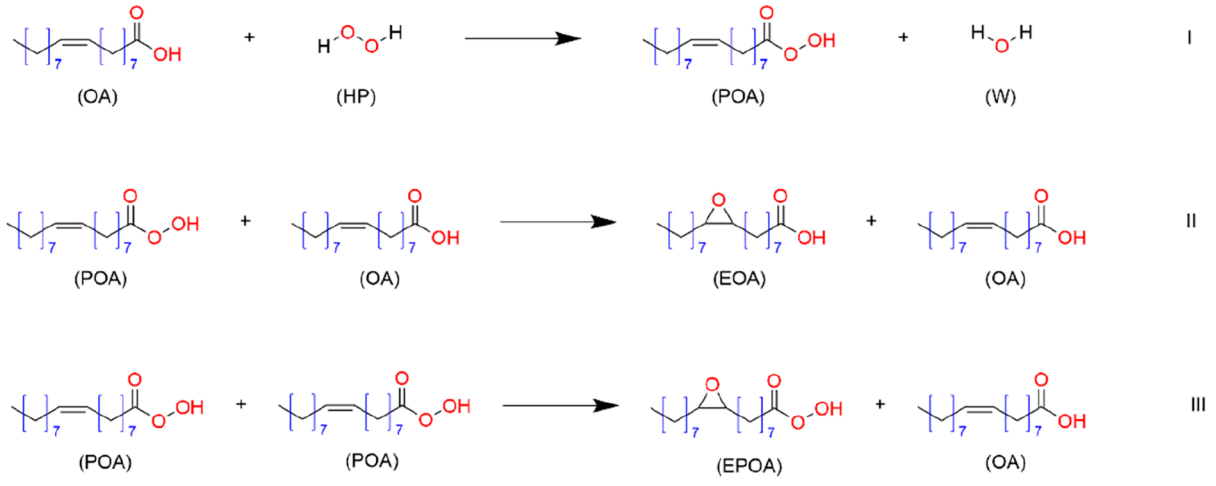

Figure 15. Stoichiometry for chemo-enzymatic epoxidation via percarboxylic acid route.

https://doi.org/10.1021/acs.iecr.3c00890
Ind. Eng. Chem. Res. 2023, 62, 9169−9187

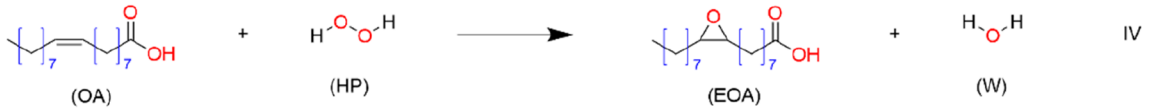

Figure 16. Stoichiometry for direct epoxidation of unsaturated fatty acid.

Table 4. Mechanistic Sequence for the Kinetic Model

no.	reaction step	
	Adsorption	
1	HP + ∗ ⇄ HP*	
2	OA + ∗ ⇄ OA*	
3	POA + ∗ ⇄ POA*	
4	W + ∗ ⇄ W*	
	Surface Reaction	
5	OA* + HP* → POA* + W*	(rds I)
6	POA* + OA* → EOA* + OA*	(rds II)
7	POA* + POA* → EPOA* + OA*	(rds III)
	Desorption	
8	EOA* ⇄ EOA + ∗	
9	EPOA* ⇄ EPOA + ∗	
	Overall Reactions	
10	OA + HP → POA + W	(I)
11	POA + OA → EOA + OA	(II)
12	POA + POA → EPOA + OA	(III)

$$\theta_v = \frac{1}{1 + \sum K_i c_i} \tag{6}$$

This equation is used with eq 4, resulting in an equation for each respective fraction of absorbed molecule on the active catalyst sites (θ_i):

$$\theta_i = \frac{K_i c_i}{1 + \sum K_i c_i} \tag{7}$$

Inserting eq 7 into the rate equations (eqs 1−3) gives the following rate expressions:

$$r_I = \frac{k_I K_{OA} K_{HP} c_{OA} c_{HP}}{(1 + \sum K_i c_i)^2} \tag{8}$$

$$r_{II} = \frac{k_{II} K_{OA} K_{POA} c_{OA} c_{POA}}{(1 + \sum K_i c_i)^2} \tag{9}$$

$$r_{III} = \frac{k_{III} K_{POA}{}^2 c_{POA}{}^2}{(1 + \sum K_i c_i)^2} \tag{10}$$

For a more compact form, the adsorption equilibrium constants (K_i) and the rate constants (k_i) can be merged into a constant k_i', resulting in

$$r_I = \frac{k_I' c_{OA} c_{HP}}{(1 + \sum K_i c_i)^2} \tag{11}$$

$$r_{II} = \frac{k_{II}' c_{OA} c_{POA}}{(1 + \sum K_i c_i)^2} \tag{12}$$

$$r_{III} = \frac{k_{III}' c_{POA}{}^2}{(1 + \sum K_i c_i)^2} \tag{13}$$

where

$$\sum K_i c_i = K_{OA} c_{OA} + K_{POA} c_{POA} + K_{EOA} c_{EOA} + K_{EPOA} c_{EPOA} + K_{HP} c_{HP} + K_W c_W$$

for i = OA, POA, EOA, EPOA, HP, and W.

Assuming low adsorption for everything except unsaturated fatty acid, hydrogen peroxide, and epoxide results in the following approximation:

$$\sum K_i c_i = K_{OA} c_{OA} + K_{HP} c_{HP} + K_{EOA} c_{EOA}$$

Ring-opening reactions have been observed in several previous studies.[15,41,42] Ring opening was also observed in this work through experimental results and confirmed by NMR analysis. For the model to be able to describe quantitatively the reaction kinetics, the ring-opening products and their rates must be taken into consideration. The kinetics for the ring opening was assumed to be

$$r_{ROP_i} = k_{ROP} c_{OA} c_i \tag{14}$$

where i = EOA or EPOA. The oleic acid concentration is included in the rate equation because ring opening is an acid-catalyzed process.[16]

The final generation rate for each component can then be calculated by taking the stoichiometry into account:

$$r_{OA} = -r_I + r_{III} - r_{ROP_{EOA}} - r_{ROP_{EPOA}} \tag{15}$$

$$r_{POA} = r_I - r_{II} - 2r_{III} \tag{16}$$

$$r_{EOA} = r_{II} - r_{ROP_{EOA}} \tag{17}$$

$$r_{EPOA} = r_{III} - r_{ROP_{EPOA}} \tag{18}$$

$$r_{HP} = -r_I \tag{19}$$

$$r_W = r_I \tag{20}$$

4.3. Component Mass Balances in Semibatch and Batch Reactors. Interfacial mass transfer between the aqueous and organic phases is of high importance in a liquid−liquid−solid system. It is presumed that the epoxidation reaction takes place in the organic phase adjacent to the catalyst particles, whereas the perhydrolysis takes place in the bulk of the aqueous phase.[16,50] For this reason, the mass balances are divided according to the reaction phase. The droplets of organic phase are assumed to be completely dispersed in the aqueous phase. The solubilities of the fatty acid and the epoxide in the aqueous phase are, however, considered to be negligible, whereas hydrogen peroxide is distributed between the two phases.

The distribution coefficient (K_{D_i}) for a specific component between the aqueous and organic phases is defined by

$$K_{D_i} = \frac{c_{ai}}{c_{oi}} \tag{21}$$

Due to rapid interfacial mass transfer compared to intrinsic reaction kinetics, the bulk-phase concentrations in the aqueous phase (a) and organic phase (o) can be used in eq 21.

https://doi.org/10.1021/acs.iecr.3c00890
Ind. Eng. Chem. Res. 2023, 62, 9169−9187

The catalyst bulk density is defined as the mass of catalyst divided by the volume of the organic phase:

$$\rho_{cat} = \frac{m_{cat}}{V_o} \tag{22}$$

The phase ratio (α) is defined as

$$\alpha = \frac{V_a}{V_a + V_o} \tag{23}$$

which can be rewritten as

$$\frac{V_a}{V_o} = \frac{\alpha}{1-\alpha} \tag{24}$$

A vigorously stirred liquid−liquid−solid three-phase semibatch reactor is considered in this section. The batch reactor model is obtained as a special case of the semibatch reactor model. Hydrogen peroxide and water still coexist in the organic and aqueous phases, but a continuous feed of the aqueous solution of hydrogen peroxide is taken into account. Hence, the mass balance for the aqueous phase (a) can be written as

$$\dot{n}_{ai} = N_i A + \frac{dn_{ai}}{dt} \tag{25}$$

and for the organic phase (o) we obtain

$$N_i A + r_i m_{cat} = \frac{dn_{oi}}{dt} \tag{26}$$

where i = HP or W, A stands for the interfacial area between the two phases, $\dot{n}_i$ is the molar flow rate of component i, and m_{cat} is the mass of catalyst. The chemical reactions are significantly slower than the interfacial mass transfer, enabling the combination of eqs 25 and 26 to obtain

$$r_i m_{cat} = \frac{dn_{ai}}{dt} + \frac{dn_{oi}}{dt} - \dot{n}_{ai} \tag{27}$$

This can be rewritten to be expressed with the component concentrations and volume. However, unlike the batch model, the volume of the aqueous phase does not remain constant, which results in the following expressions:

$$\frac{dn_{ai}}{dt} = V_a \frac{dc_{ai}}{dt} + c_{ai}\frac{dV_a}{dt} \tag{28}$$

$$\frac{dn_{oi}}{dt} = V_o \frac{dc_{oi}}{dt} \tag{29}$$

Because of the constant feed rate, the volume of the aqueous phase at any given time can be described as

$$V_a = V_{0a} + \dot{V}_a t \tag{30}$$

where V_{0a} is the initial liquid volume of the aqueous phase and $\dot{V}_a$ is the volume flow rate of the aqueous feed. Hence, the time derivative of the aqueous liquid phase becomes

$$\frac{dV_a}{dt} = \dot{V}_a \tag{31}$$

By inserting eqs 30 and 31 into eq 28 we obtain

$$\frac{dn_{ai}}{dt} = V_a \frac{dc_{ai}}{dt} + c_{ai}\dot{V}_a \tag{32}$$

Introducing eqs 29 and 32 into eq 27 and taking the distribution coefficient (K_{D_i}) into account result in the following expression:

$$V_a \frac{dc_{ai}}{dt} + c_{ai}\dot{V}_a + V_o \frac{dc_{ai}}{K_{D_i} dt} - \dot{n}_{ai} = r_i m_{cat} \tag{33}$$

The relationship between molar flow rate and concentration can be described as

$$\dot{n}_{ai} = c_{0ai}\dot{V}_a \tag{34}$$

where c_{0ai} is the concentration of the aqueous feed. Inserting eq 34 and the catalyst bulk density from eq 22 into eq 33 results in

$$\frac{dc_{ai}}{dt} = \frac{r_i \rho_{cat} + \left(\frac{c_{0ai}\dot{V}_a - c_{ai}\dot{V}_a}{V_o}\right)}{V_a/V_o + 1/K_{D_i}} \tag{35}$$

Introducing the phase ratio (α) from eq 24 gives us the final expression

$$\frac{dc_{ai}}{dt} = \frac{(1-\alpha)\left[r_i \rho_{cat} + \left(\frac{c_{0ai}\dot{V}_a - c_{ai}\dot{V}_a}{V_o}\right)\right]}{\alpha + (1-\alpha)/K_{D_i}} \tag{36}$$

Following an analogous reasoning for the time derivative of the organic phase culminates in

$$\frac{dc_{oi}}{dt} = \frac{(1-\alpha)\left[r_i \rho_{cat} + \left(\frac{c_{0ai}\dot{V}_a - c_{ai}\dot{V}_a}{V_o}\right)\right]}{\alpha K_{D_i} + 1 - \alpha} \tag{37}$$

Equations 36 and 37 are applicable for the compounds that are present in both phases, i.e., hydrogen peroxide and water. For the compounds that are nonsoluble in the aqueous phase, i.e., oleic acid and the epoxide, $K_{D_i} = 0$ in eq 37 and eq 36 is omitted.

The batch reactor model is obtained as a special case of the semibatch model by setting the volumetric flow rate $\dot{V}_a = 0$ in eqs 36 and 37. The effect of sampling on the total volume was evaluated and included in the model, because the bulk density of the catalyst depends on liquid volume, i.e., $\rho_{cat} = m_{cat}/V_0 = m_{cat}/(V_{0o} - \sum V_{sample})$. Before the parameter estimation, the impact of internal diffusion was evaluated by using the standard criterion (Weisz−Prater) for the system. The catalyst porosity and tortuosity were assumed to be 0.5 and 6, respectively, according to information from the literature.[51] Because of the relatively small particle size (radius = 0.33 mm) and low reaction rate, the internal diffusion resistance was confirmed to be negligible.

4.4. Parameter Estimation Procedure and Results. Based on the experimental data collected in this work, parameter estimation was conducted. The concentrations of epoxide and double bonds were determined from the oxirane and iodine value analyses performed for the organic phase, whereas the hydrogen peroxide concentration was determined through titration of the aqueous phase. The parameters were estimated by minimizing the sum of squared residuals from the experimental and estimated values with the following equation:

$$Q = \sum_i \sum (y_{i,exp} - y_{i,th})^2 \tag{38}$$

where Q refers to the objective function, $y_{i,exp}$ is the experimental value, and $y_{i,th}$ is the value estimated by the model. The concentrations needed in calculating $y_{i,th}$ were obtained by numerical solution of the mass balances in eqs 36 and 37 during the parameter estimation.

To determine the parameters the model, computations and estimations were done using the ModelingToolkit[52] and

https://doi.org/10.1021/acs.iecr.3c00890
Ind. Eng. Chem. Res. 2023, 62, 9169−9187

LsqFit[53] packages in the programming language Julia.[54] The ordinary differential equations given by eqs 36 and 37 were solved using the Rosenbrock method,[55] and for finding the minimum of the objective function, the Levenberg−Marquardt algorithm[56,57] was used. Standard statistical analysis was applied to the kinetic parameters, i.e., the variances of the parameters were calculated from the structural matrix and the objective function given in eq 38.[58] The sensitivity analysis of the parameters was done by varying the value of one parameter while keeping the values of the other parameters at the optima which were obtained by minimizing the objective function.[58] This procedure was repeated for each parameter.

In total, 10 unknown parameters were estimated using the data collected from the experiments. Experimental points which were obvious outliers due to experimental errors or mistakes in the chemical analysis were removed to achieve a better fit. In total, 13 experiments with fresh catalysts were used for the parameter estimation (Table 1, experiments 1−13). The parameters estimated were the rate constants for all the reactions(k_i'), the rate constants for ring-opening reactions (k_{ROP_i}), the adsorption equilibrium constants for hydrogen peroxide (K_{HP}), oleic acid (K_{OA}), and epoxidized oleic acid (K_{EOA}), and finally the distribution coefficients K_{D_i} for the compounds present in both phases. A collection of the estimated parameters and their errors as well as the parameters which were kept constant can be seen in Table 5, and the sensitivity analysis for the parameters is presented in Figure 17.

Table 5. Estimated Parameters

parameter	value	estimated/ fixed	std. error	relative std. error (%)
k_I'	4.34×10^{-4}	estimated	6.45×10^{-5}	14.9
k_{II}'	2.38×10^{-2}	fixed	N/A	N/A
k_{III}'	0	fixed	N/A	N/A
$k_{ROP_{EOA}}$	6.49×10^{-6}	estimated	4.46×10^{-7}	6.9
$k_{ROP_{EPOA}}$	0	fixed	N/A	N/A
K_{OA}	6.44×10^{-1}	estimated	7.70×10^{-2}	12.0
K_{HP}	2.48×10^{-1}	estimated	3.27×10^{-2}	13.2
K_{EOA}	0	fixed	N/A	N/A
$K_{D_{HP}}$	10^5	fixed	N/A	N/A
K_{D_W}	10^5	fixed	N/A	N/A

The parameter estimation gave an indication that the formation of epoxidized peroleic acid and consequently its ring opening were negligible. For this reason, the rate constants k_{III}' and $k_{ROP_{EPOA}}$ were fixed to zero. Additionally, the distribution coefficients K_{D_i} for hydrogen peroxide and water were assumed to be extremely high and therefore were set as a high constant. The adsorption equilibrium constant for the product K_{EOA} went toward zero in the estimations and because of that was set as constant. The possibility of catalyst deactivation during the long experiments exists, as indicated by the catalyst recycle studies (Figure 10), but as a first approximation, this effect was discarded in the parameter estimation.

From the estimation and sensitivity analysis, it was observed that the epoxidation reaction was significantly faster than the perhydrolysis, confirming that perhydrolysis is the rate-determining step. Because of this, the rate constant k_{II}' only had a minimum value for the estimation and an infinite maximum. As a consequence, it was decided to use a value from

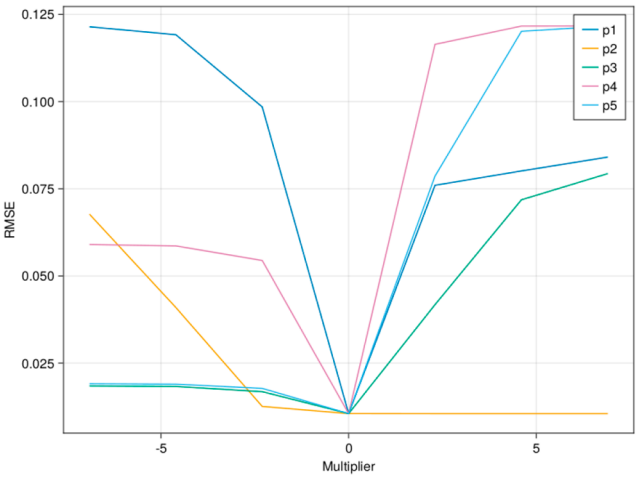

Figure 17. Sensitivity analysis. p1 = k_I', p2 = k_{II}', p3 = $k_{ROP_{EOA}}$, p4 = K_{OA}, and p5 = K_{HP}.

our previous work[50] that was above the minimum. Overall, a good fit was achieved for the coefficient of determination (R^2) exceeding 98% and a root-mean-square error (RMSE) of 1.05×10^{-2}. The estimated fits to experimental data for some examples can be seen in Figures 18 and 19.

In the semibatch experiments with high molar ratios of hydrogen peroxide to oleic acid, sort of an S-curve pattern could be seen for the hydrogen peroxide concentration. This was assumed to be caused by the decomposition of hydrogen peroxide into water and oxygen, resulting in oxygen being pumped when the syringe was close to empty. However, from the model fitting of experimental data, it can be seen that the model mimics the same behavior, which can be seen in Figure 18D and Figure 19F. A plausible explanation for this behavior is rather that the oleic acid and hydrogen peroxide react for the first half of the experiment, resulting in the consumption of hydrogen peroxide, followed by the accumulation of hydrogen peroxide due to the oleic acid having mostly been consumed.

The kinetic model developed was applied to different molar ratios of the reactants and different operation policies (batch and semibatch). The possible catalyst deactivation was not included in the kinetic model, but in spite of this simplification, a good description of the experimental data was achieved. In order to further investigate the predictability of the model, experiments at various temperatures could be done to reveal the temperature dependences of the rate parameters, which steer the product distribution of epoxides and ring-opening products.

5. CONCLUSIONS AND FUTURE PERSPECTIVES

Enzymatic epoxidation of unsaturated fatty acids was successfully performed in this work, achieving a good conversion of double bonds and high yields of epoxide under mild conditions. A rotating bed reactor was used as a stirring device and demonstrated good results for forming the emulsion and being gentle on the immobilized lipase catalyst.

The double bond conversion and reaction rate are significantly affected by the amount of hydrogen peroxide compared to fatty acid. The application of the semibatch technology with gradual addition of hydrogen peroxide resulted in higher epoxidation yields due to better selectivity with a suppressed prevalence of ring-opening reactions, which was confirmed with NMR analysis. The catalyst deactivation and

https://doi.org/10.1021/acs.iecr.3c00890
Ind. Eng. Chem. Res. 2023, 62, 9169−9187

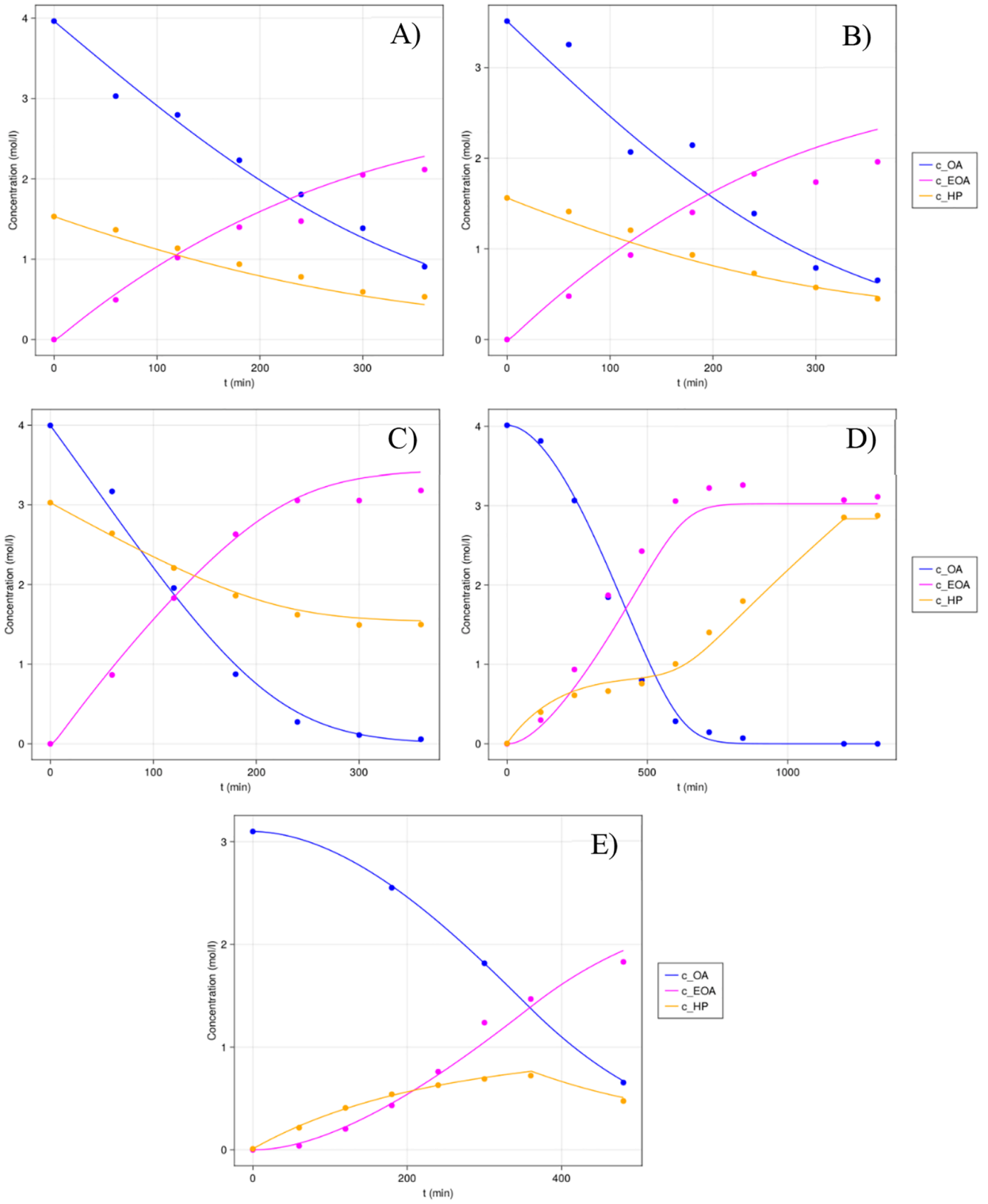

Figure 18. Model fitted to experimental data. Lines show computed values, and dots show experimental data. Color code: (blue) oleic acid (OA); (yellow) hydrogen peroxide (HP); (magenta) epoxidized oleic acid (EOA). Experimental conditions: T = 50 °C; stirring rate = 1000 rpm; catalyst loading = 7%; OA:HP molar ratio = (A, B, E) 1:1, (C) 1:2, (D) 1:3. Modes: (A−C) batch; (D) semibatch, 20 h addition time; (E) semibatch, 6 h addition time.

https://doi.org/10.1021/acs.iecr.3c00890
Ind. Eng. Chem. Res. 2023, 62, 9169−9187

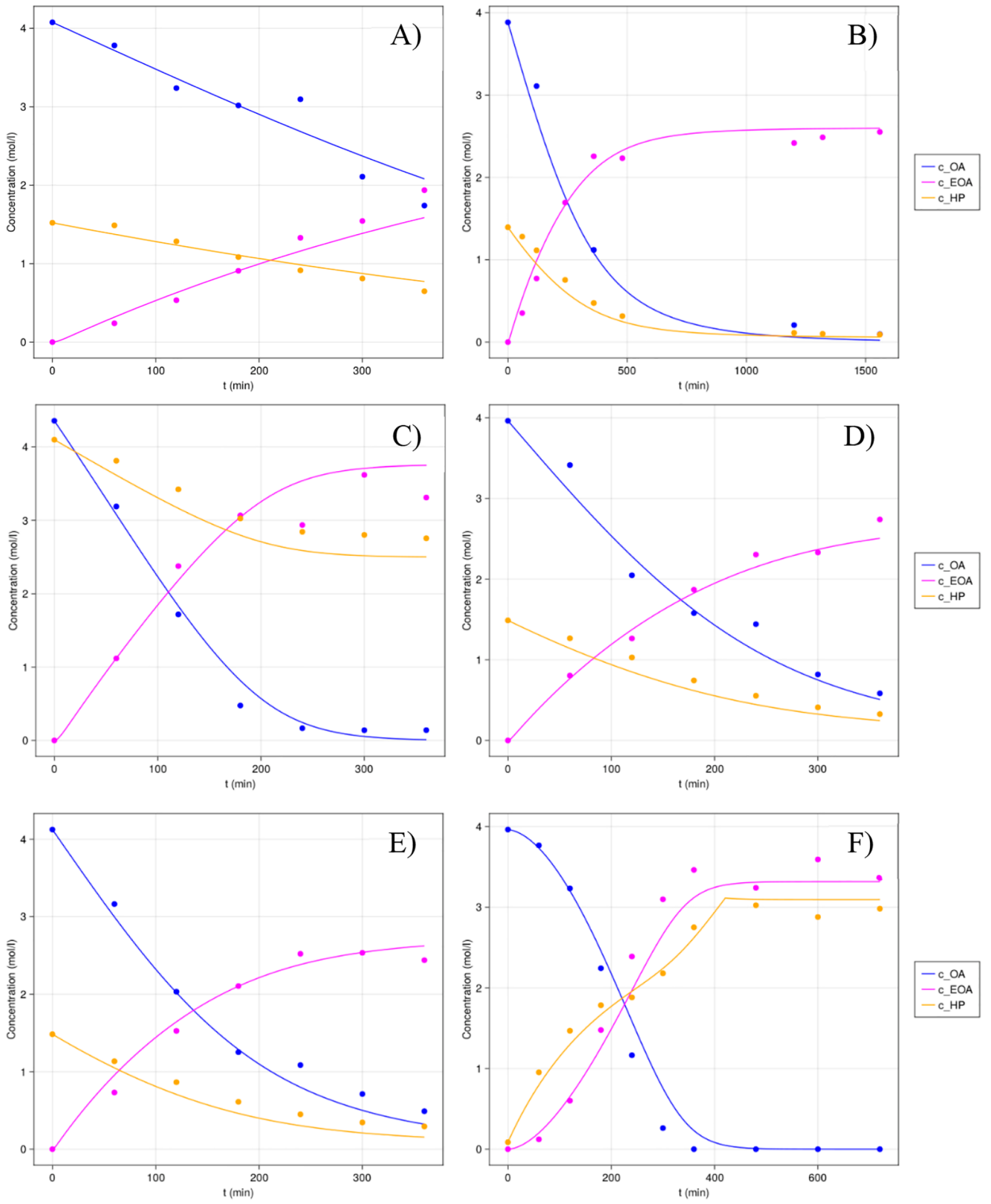

Figure 19. Model fitted to experimental data. Lines show computed values, and dots show experimental data. Color code: (blue) oleic acid (OA); (yellow) hydrogen peroxide (HP); (magenta) epoxidized oleic acid (EOA). Experimental conditions: T = 50 °C; stirring rate = 1000 rpm; catalyst loading = (A) 4%, (B–D, F) 7%, (E) 13%; OA:HP molar ratio = (A, B, D, E) 1:1, (C, F) 1:3. Modes: (A–E) batch; (F) semibatch, 7 h addition time.

reusability were studied by reusing the catalyst in successive experiments with washes in between. Pretreatment of the catalyst with hydrogen peroxide had a deteriorating effect on its activity. A clearly lower surface area was observed for the used

https://doi.org/10.1021/acs.iecr.3c00890
Ind. Eng. Chem. Res. 2023, 62, 9169–9187

catalyst compared to the fresh one. This is likely caused by ring-opening products blocking the catalyst pores. The observation agrees with the results from the NMR analysis, which confirmed that the utilization of semibatch mode suppresses the ring-opening reactions.

A mathematical model based on elementary reaction steps for the semibatch system was developed, and parameter estimation was successfully performed using the collected kinetic data. The parameter estimation indicated that the perhydrolysis step is the rate-determining one, with the epoxidation step being significantly faster. Overall, a good fit was achieved between the model predictions and the experimental data. Several kinetic parameters were estimated with a reasonable accuracy.

For future investigations, additional experiments at different temperatures could be conducted and a more thorough study of catalyst deactivation could be performed, where the catalyst can be reused for an extensive number of experiments replicating industrial practices. Furthermore, other causes of deactivation could be investigated, for example, the deposition of byproducts on the catalyst structure, enzyme leaching, and the role of hydrogen peroxide in inhibiting the enzymatic sites. Lastly, a system using the enzymatic method in a continuous bed reactor would be an interesting option.

■ ASSOCIATED CONTENT

Supporting Information

The Supporting Information is available free of charge at https://pubs.acs.org/doi/10.1021/acs.iecr.3c00890.

Molecular structures, chemicals, aqueous phase analysis, organic phase analysis, ^{1}H NMR spectra of oleic acids, and SEM images of catalyst particles (PDF)

■ AUTHOR INFORMATION

Corresponding Author

Tapio Salmi − *Laboratory of Industrial Chemistry and Reaction Engineering (TKR), Johan Gadolin Process Chemistry Centre (PCC), Åbo Akademi University, FI-20500 Turku/Åbo, Finland;* orcid.org/0000-0002-9271-7425; Email: tapio.salmi@abo.fi

Authors

Wilhelm Wikström − *Laboratory of Industrial Chemistry and Reaction Engineering (TKR), Johan Gadolin Process Chemistry Centre (PCC), Åbo Akademi University, FI-20500 Turku/Åbo, Finland*

Adriana Freites Aguilera − *Laboratory of Industrial Chemistry and Reaction Engineering (TKR), Johan Gadolin Process Chemistry Centre (PCC), Åbo Akademi University, FI-20500 Turku/Åbo, Finland*

Pasi Tolvanen − *Laboratory of Industrial Chemistry and Reaction Engineering (TKR), Johan Gadolin Process Chemistry Centre (PCC), Åbo Akademi University, FI-20500 Turku/Åbo, Finland;* orcid.org/0000-0003-0462-1421

Robert Lassfolk − *Laboratory of Industrial Chemistry and Reaction Engineering (TKR), Johan Gadolin Process Chemistry Centre (PCC), Åbo Akademi University, FI-20500 Turku/Åbo, Finland;* orcid.org/0000-0002-6555-3488

Ananias Medina − *Laboratory of Industrial Chemistry and Reaction Engineering (TKR), Johan Gadolin Process Chemistry Centre (PCC), Åbo Akademi University, FI-20500 Turku/Åbo, Finland;* orcid.org/0000-0002-7227-7645

Kari Eränen − *Laboratory of Industrial Chemistry and Reaction Engineering (TKR), Johan Gadolin Process Chemistry Centre (PCC), Åbo Akademi University, FI-20500 Turku/Åbo, Finland*

Complete contact information is available at: https://pubs.acs.org/10.1021/acs.iecr.3c00890

Notes

This work is based on the experimental material of the Master's thesis of W.W. at Åbo Akademi University, available at: https://www.doria.fi/bitstream/handle/10024/186642/wikstr%C3%B6m_wilhelm.pdf.

The authors declare no competing financial interest.

■ ACKNOWLEDGMENTS

This work is part of the activities financed by Academy of Finland through the Academy Professor Grants 319002, 320115, and 345053 (T.S. and A.F.A.). Economic support from Åbo Akademi Foundation (Walter Qvist Scholarship to Wilhelm Wikström) is gratefully acknowledged. Mark Martinez Klimov and Linus Silvander are acknowledged for the surface area measurements and SEM investigations. We are grateful to SpinChem AB for providing the mixing device to our disposal.

■ NOTATION

List of Symbols

A = interfacial mass transfer area (m^2)
c_i = molar concentration (mol/L)
IV = iodine value
IV_0 = initial iodine value
k_i' = merged rate constant
k_i = kinetic rate constant (min^{-1})
K_i = equilibrium constant
K_{D_i} = distribution coefficient
m_i = mass (g)
m_{cat} = mass of catalyst (g)
MM_i = molar mass (g/mol)
n_i = amount of substance (mol)
$\dot{n}_i$ = molar flow rate (mol/min)
N_i = molar flux (mol min^{-1} m^{-2})
OO_{exp} = experimentally determined oxirane oxygen (mol/100 g of oil)
OO_{th} = theoretical maximum of oxirane oxygen (mol/100 g of oil)
PLU/g = propyl laurate unit per gram (enzyme activity per gram)
Q = objective function
r_i = generation rate
V_i = volume (L)
$\dot{V}_i$ = volumetric flow rate (L/min)
$y_{i,exp}$ = experimentally obtained value
$y_{i,th}$ = value computed by the model
α = phase ratio
θ_i = fraction of adsorbed molecules on active surface sites
θ_v = fraction of vacant surface sites
ρ_{cat} = catalyst bulk density (g/L of organic phase)

Abbreviations

B = batch
BET = Brunauer−Emmett−Teller
Cat = catalyst
CTO = crude tall oil
DB = double bond

https://doi.org/10.1021/acs.iecr.3c00890
Ind. Eng. Chem. Res. 2023, 62, 9169−9187

EOA = epoxidized oleic acid
EPOA = epoxidized peroleic acid
HP = hydrogen peroxide
N/A = not available
NMR = nuclear magnetic resonance spectroscopy
OA = oleic acid
OO = oxirane oxygen
PLU = propyl laurate unit
POA = peroleic acid
RBR = rotating bed reactor
RCO = relative conversion to oxirane (%) (minimum 0%, maximum = 100%)
RCU = relative concentration of double bonds (%) (100% at t = 0, minimum 0% at full conversion)
rds = rate-determining step
ROP = ring-opening product
RPM = revolutions per minute
SB = semibatch
SEM = scanning electron microscopy
TOFA = tall oil fatty acid
W = water
wt % = weight percent
% w/v = percent weight by volume
% w/w = percent weight by weight

REFERENCES

(1) Rosillo-Calle, F.; Pelkmans, L.; Walter, A. *A Global Overview of Vegetable Oils, with Reference to Biodiesel*; IEA Bioenergy, 2009.
(2) Jalil, M. J.; Hadi, A.; Azmi, I. S. Catalytic epoxidation of palm oleic acid using in situ generated performic acid − optimization and kinetic studies. *Mater. Chem. Phys.* **2021**, *270*, 124754.
(3) Piccolo, D.; Vianello, C.; Lorenzetti, A.; Maschio, G. Epoxidation of soybean oil enhanced by microwave radiation. *Chem. Eng. J.* **2019**, *377*, 120113.
(4) Danov, S. M.; Kazantsev, O. A.; Esipovich, A. L.; Belousov, A. S.; Rogozhin, A. E.; Kanakov, E. A. Recent advances in the field of selective epoxidation of vegetable oils and their derivatives: A review and perspective. *Catal. Sci. Technol.* **2017**, *7* (17), 3659−3675.
(5) Saurabh, T.; Patnaik, M.; Bhagt, S. L.; Renge, V. C. Epoxidation of vegetable oils: a review. *Int. J. Adv. Eng. Technol.* **2011**, *2*, 491−501.
(6) Gan, L. H.; Ooi, K. S.; Goh, S. H.; Gan, L. M.; Leong, Y. C. Epoxidized esters of palm olein as plasticizers for poly(vinyl chloride). *Eur. Polym. J.* **1995**, *31* (8), 719−724.
(7) Adhvaryu, A.; Erhan, S. Z. Epoxideized soybean oil as potential source of high temperature lubricants. *Ind. Crops Prod.* **2002**, *15* (3), 247−254.
(8) Tan, S. G.; Chow, W. S. Biobased epoxidized vegetable oils and its greener epoxy blends: a review. *Polym.-Plast. Technol. Eng.* **2010**, *49* (15), 1581−1590.
(9) Aryan, V.; Kraft, A. The crude tall oil value chain: Global Availability and the influence of regional energy policies. *J. Cleaner Prod.* **2021**, *280*, 124616.
(10) Mongkhonsiri, G.; Gani, R.; Malakul, P.; Assabumrungrat, S. Integration of the biorefinery concept development of sustainable processes for pulp and Paper Industry. *Comput. Chem. Eng.* **2018**, *119*, 70−84.
(11) Gamage, P. K.; O'Brien, M.; Karunanayake, L. Epoxidation of some vegetable oils and their hydrolysed products with peroxyformic acid − optimized to industrial scale. *J. Natl. Sci. Found. Sri Lanka* **2009**, *37* (4), 229.
(12) Logan, L. R. Tall oil fatty acids. *J. Am. Oil Chem. Soc.* **1979**, *56*, 777A−779A.
(13) Prileschajew, N. Oxydanation ungesättigter Verbindungen Mittels Organischer Superoxyde. *Ber. Dtsch. Chem. Ges.* **1909**, *42* (4), 4811−4815.
(14) Leveneur, S.; Ledoux, A.; Estel, L.; Taouk, B.; Salmi, T. Epoxidation of vegetable oils under microwave irradiation. *Chem. Eng. Res. Des.* **2014**, *92* (8), 1495−1502.
(15) Freites Aguilera, A.; Tolvanen, P.; Eränen, K.; Leveneur, S.; Salmi, T. Epoxidation of oleic acid under conventional heating and microwave radiation. *Chem. Eng. Process.* **2016**, *102*, 70−87.
(16) Freites Aguilera, A.; Tolvanen, P.; Eränen, K.; Wärnå, J.; Leveneur, S.; Marchant, T.; Salmi, T. Kinetic modelling of Prileschajew epoxidation of oleic acid under conventional heating and microwave irradiation. *Chem. Eng. Sci.* **2019**, *199*, 426−438.
(17) Dinda, S.; Patwardhan, A. V.; Goud, V. V.; Pradhan, N. C. Epoxidation of cottonseed oil by aqueous hydrogen peroxide catalysed by liquid inorganic acids. *Bioresour. Technol.* **2008**, *99* (9), 3737−3744.
(18) Petrović, Z. S.; Zlatanić, A.; Lava, C. C.; Sinadinović-Fišer, S. Epoxidation of soybean oil in toluene with peroxoacetic and peroxoformic acids − kinetics and side reactions. *Eur. J. Lipid Sci. Technol.* **2002**, *104* (5), 293−299.
(19) Sinadinović-Fišer, S.; Janković, M.; Petrović, Z. S. Kinetics of in situ epoxidation of soybean oil in bulk catalyzed by ion exchange resin. *J. Am. Oil Chem. Soc.* **2001**, *78* (7), 725−731.
(20) Sinadinović-Fišer, S.; Janković, M.; Borota, O. Epoxidation of castor oil with peracetic acid formed in situ in the presence of an ion exchange resin. *Chem. Eng. Process.* **2012**, *62*, 106−113.
(21) Campanella, A.; Baltanás, M. A.; Capel-Sánchez, M. C.; Campos-Martin, J. M.; Fierro, J. L. Soybean oil epoxidation with hydrogen peroxide using amorphous Ti/SiO_2 catalyst. *Green Chem.* **2004**, *6* (7), 330−334.
(22) Cai, S. F.; Wang, L.-S.; Fan, C.-L. Catalytic epoxidation of a technical mixture of methyl oleate and methyl linoleate in ionic liquids using $MoO(O_2)_2{\cdot}2QOH$ (QOH = 8-quinilinol) as catalyst and $NaHCO_3$ as co-catalyst. *Molecules* **2009**, *14* (8), 2935−2946.
(23) Gerbase, A. E.; Gregório, J. R.; Martinelli, M.; Brasil, M. C.; Mendes, A. N. Epoxidation of soybean oil by the methyltrioxorhenium-$CHCl_2/H_2O_2$ catalytic biphasic system. *J. Am. Oil Chem. Soc.* **2002**, *79* (2), 179−181.
(24) Curci, R.; Fiorentino, M.; Troisi, L.; Edwards, J. O.; Pater, R. H. Epoxidation of alkenes by dioxirane intermediates generated in the reaction of potassium caroate with ketones. *J. Org. Chem.* **1980**, *45* (23), 4758−4760.
(25) Gao, C.-J.; Shin, W.-S.; Han, J.-M.; Han, D.-Y.; Adharvana Chari, M.; Kim, H.-D.; Ahn, K.-H. Green epoxidation of olefins catalyzed by carbon dioxide soluble chiral Salen-Mn(III) complexes in Supercritical CO_2. *Bull. Korean Chem. Soc.* **2009**, *30* (3), 541−542.
(26) Björkling, F.; Godtfredsen, S. E.; Kirk, O. Lipase-mediated formation of percarboxylic acids used in catalytic epoxidation of alkenes. *J. Chem. Soc., Chem. Commun.* **1990**, *19*, 1301−1303.
(27) Warwel, S.; Rüsch gen. Klaas, M. Chemo-enzymatic epoxidation of unsaturated carboxylic acids. *J. Mol. Catal. B: Enzym.* **1995**, *1* (1), 29−35.
(28) Rüsch gen. Klaas, M.; Warwel, S. Complete and partial epoxidation of plant oils by lipase-catalyzed perhydrolysis. *Ind. Crops Prod.* **1999**, *9* (2), 125−132.
(29) Yadav, G. D.; Manjula Devi, K. A kinetic model for the enzyme-catalyzed self-epoxidation of oleic acid. *J. Am. Oil Chem. Soc.* **2001**, *78* (4), 347−351.
(30) Biermann, U.; Friedt, W.; Lang, S.; Lühs, W.; Machmüller, G.; Metzger, J. O.; Rüsch gen. Klaas, M.; Schäfer, H. J.; Schneider, M. P. New syntheses with oils and fats as renewable raw material for the chemical industry. *Angew. Chem., Int. Ed.* **2000**, *39* (13), 2206−2224.
(31) Sun, S.; Ke, X.; Cui, L.; Yang, G.; Bi, Y.; Song, F.; Xu, X. Enzymatic epoxidation of Sapindus mukorossi seed oil by perstearic acid optimized using response surface methodology. *Ind. Crops Prod.* **2011**, *33* (3), 676−682.
(32) Sun, S.; Shan, L.; Liu, Y.; Jin, Q.; Song, Y.; Wang, X. Solvent-free enzymatic synthesis of feruloylated diacylglycerols and kinetic study. *J. Mol. Catal. B: Enzym.* **2009**, *57* (1−4), 104−108.
(33) Hilker, I.; Bothe, D.; Prüss, J.; Warnecke, H. J. Chemo-enzymatic epoxidation of unsaturated plant oils. *Chem. Eng. Sci.* **2001**, *56* (2), 427−432.

https://doi.org/10.1021/acs.iecr.3c00890
Ind. Eng. Chem. Res. 2023, 62, 9169−9187

(34) Törnvall, U.; Orellana-Coca, C.; Hatti-Kaul, R.; Adlercreutz, D. Stability of immobilized *Candida antarctica* lipase B during chemo-enzymatic epoxidation of fatty acids. *Enzyme Microb. Technol.* **2007**, *40* (3), 447−451.
(35) Aouf, C.; Durand, E.; Lecomte, J.; Figueroa-Espinoza, M.-C.; Dubreucq, E.; Fulcrand, H.; Villeneuve, P. The use of lipases as biocatalysts for the epoxidation of fatty acids and phenolic compounds. *Green Chem.* **2014**, *16* (4), 1740−1754.
(36) Hagström, A. E.; Törnvall, U.; Nordblad, N.; Hatti-Kaul, R.; Woodley, J. M. Chemo-enzymatic epoxidation-process options for improving biocatalytic productivity. *Biotechnol. Prog.* **2011**, *27* (1), 67−76.
(37) Anastas, P.; Eghbali, N. Green Chemistry: Principles and practice. *Chem. Soc. Rev.* **2010**, *39* (1), 301−312.
(38) Orellana-Coca, C.; Törnvall, U.; Adlercreutz, D.; Mattiasson, B.; Hatti-Kaul, R. Chemo-enzymatic epoxidation of oleic acid and methyl oleate in solvent-free medium. *Biocatal. Biotransform.* **2005**, *23* (6), 431−437.
(39) Zhang, X.; Wan, X.; Cao, H.; Dewil, R.; Deng, L.; Wang, F.; Tan, T.; Nie, K. Chemo-enzymatic epoxidation of Sapindus Mukurossi fatty acids catalyzed with *Candida sp*. 99−125 lipase in a solvent-free system. *Ind. Crops Prod.* **2017**, *98*, 10−18.
(40) Freites Aguilera, A.; Tolvanen, P.; Sifontes Herrera, V.; Tourvielle, J.-N.; Leveneur, S.; Salmi, T. Reaction intensification by microwave and ultrasound techniques in chemical multiphase systems. In *Process Synthesis and Process Intensification: Methodological Approches*; Rong, B.-G., Ed.; De Gruyter, 2017; 111−142.
(41) Freites Aguilera, A.; Lindroos, P.; Rahkila, J.; Martinez Klimov, M.; Tolvanen, P.; Salmi, T. Salmi, Lipase catalyzed green epoxidation of oleic acid using ultrasound as a process intensification method. *Chem. Eng. Process.* **2022**, *174*, 108882.
(42) Freites Aguilera, A.; Tolvanen, P.; Oger, A.; Eränen, K.; Leveneur, S.; Mikkola, J.-P.; Salmi, T. Screening of ion exchange resin catalyst for epoxidation of oleic acid under the influence of conventional and microwave heating. *J. Chem. Technol. Biotechnol.* **2019**, *94* (9), 3020−3031.
(43) Mallin, H.; Muschiol, J.; Byström, E.; Bornscheuer, U. T. Efficient biocatalysis with immobilized enzymes or encapsulated whole cell microorganism by using the SpinChem Reactor System. *ChemCatChem* **2013**, *5* (12), 3529−3532.
(44) Pithani, S.; Karlsson, S.; Emtenäs, H.; Öberg, C. T. Using Spinchem rotating bed reactor technology for immobilized enzymatic reactions: A case study. *Org. Process Res. Dev.* **2019**, *23* (9), 1926−1931.
(45) Perez-Sena, W.; Wärnå, J.; Eränen, K.; Tolvanen, P.; Estel, L.; Leveneur, S.; Salmi, T. Use of semibatch reactor technology for the investigation of reaction mechanism and kinetics: Heterogeneously catalyzed epoxidation of fatty acid esters. *Chem. Eng. Sci.* **2021**, *230*, 116206.
(46) Greenspan, F. P.; MacKellar, D. G. Analysis of Aliphatic Per Acids. *Anal. Chem.* **1948**, *20* (11), 1061−1063.
(47) Kolthoff, I. M. *Chem. Weekbl.* **1920**, *17*, 197.
(48) Paquot, C. Determination of the Iodine Value (I.V.). In *Standard Methods for the Analysis of Oils, Fats and Derivatives*; Pergamon Press, 1979; pp 66−70.
(49) Jay, R. R. Direct Titration of Epoxy Compounds and Aziridines. *Anal. Chem.* **1964**, *36* (3), 667−668.
(50) Salmi, T.; Freites Aguilera, A.; Lindroos, P.; Kanerva, L. Mathematical modelling of oleic acid epoxidation via a chemo-enzymatic route − From reaction mechanism to reactor model. *Chem. Eng. Sci.* **2022**, *247*, 117047.
(51) Cordier, A.; Klinksiek, M.; Held, C.; Legros, J.; Leveneur, S. Biocatalyst and continuous microfluidic reactor for an intensified production of n-butyl levulinate: kinetic model assessment. *Chem. Eng. J.* **2023**, *451*, 138541.
(52) Ma, Y.; Gowda, S.; Anantharaman, R.; Laughman, C.; Shah, V.; Rackauckas, C. *ModelingToolkit: A Composable Graph Transformation System for Equation-Based Modeling*, 2021. https://github.com/SciML/ModelingToolkit.jl.
(53) White, J. M. *The LsqFit least-squares fitting package*, 2022. https://github.com/JuliaNLSolvers/LsqFit.jl.
(54) Julia Core Development Team. *The Julia Programming Language*, 2022. https://julialang.org/.
(55) Rosenbrock, H. H. Some general implicit processes for the numerical solution of differential equations. *Comput. J.* **1963**, *5* (4), 329−330.
(56) Levenberg, K. A method for the solution of certain non-linear problems in least squares. *Q. Appl. Math.* **1944**, *2*, 164−168.
(57) Marquardt, D. W. An Algorithm for Least-Squares Estimation of Nonlinear Parameters. *J. Soc. Ind. Appl. Math.* **1963**, *11* (2), 431−441.
(58) Salmi, T.; Wärnå, J.; Hernández Carucci, J. R.; de Araújo Filho, C. A. *Chemical Reaction Engineering. A Computer-Aided Approach*; De Gruyter: Berlin, 2020; Chapter 8, pp 139−142.

https://doi.org/10.1021/acs.iecr.3c00890
Ind. Eng. Chem. Res. 2023, 62, 9169−9187